Imaging brain aromatase by using PET

A way to study anabolic steroid abuse

Kayo Takahashi

Abstract

Aromatase is an enzyme that facilitates the conversion of androgens to estrogens and may play a role in mood and mental status. The main theme of this thesis is the imaging of brain aromatase by use of the PET technique. The PET tracer for aromatase, ^{11}C-labeled vorozole (VOZ) was developed and evaluated by with *in vitro* and *in vivo* methods. *In vitro* experiments using rat brain showed that VOZ was distributed in the medial amygdala, bed nucleus of the stria terminalis and medial preoptic area, regions of the brain known to be rich in aromatase and the K_D value was determined to be 0.60 nM. The *in vivo* PET study in rhesus monkey brain revealed that VOZ penetrated the blood-brain barrier and accumulated in the amygdala and hypothalamus. Taken together, VOZ is a good PET tracer for *in vivo* aromatase imaging with high affinity and high sensitivity.

This technique was applied to an investigation of brain aromatase under the physiological conditions simulating anabolic-androgenic steroid abuse. A significant increase in VOZ binding by anabolic-androgenic steroids was observed in the bed nucleus of stria terminalis and medial preoptic area in the rat brain. In contrast, no significant change in binding was observed in the medial amygdala. These results indicate that the manner of regulation of aromatase expression might be different in the bed nucleus of stria terminalis and medial preoptic area compared with that in the medial amygdala. The aromatase expression was suggested to be regulated through androgen receptors, as indicated in a study with flutamide treatment. The increased aromatase expression was seen in neurons. The PET study with anabolic steroid-treated rhesus monkeys also showed increased VOZ binding in the hypothalamus but not in the amygdala. The alteration of density of aromatase binding in the hypothalamic area could explain some psychological features of anabolic-androgenic steroid abusers.

Novel PET tracers for aromatase were developed and examined. The two newly synthesized ^{18}F-labeled vorozole analogs, [^{18}F]FVOZ and [^{18}F]FVOO, displayed different characteristics. Both tracers showed similar binding pattern as VOZ; however, [^{18}F]FVOO was metabolized very quickly, meaning that this tracer is not suitable as a PET tracer. On the other hand, [^{18}F]FVOZ can be an appropriate PET tracer.

The role of aromatase in the human brain has not been clarified yet. To approach this problem by *in vivo* methods, we have just started PET studies to explore aromatase expression in humans.

Keywords: aromatase, brain, molecular imaging, PET, [^{11}C]vorozole, amygdala, hypothalamus, anabolic-androgenic steroids, abuse, [^{18}F]vorozole analogs

L’esprit ne saurait jouer longtemps le personnage du cœur.

La Rochefoucauld, Maxime 108

List of papers

This thesis is based on the following papers, which are referred to in the text by their Roman numerals.

I Takahashi K, Bergström M, Frändberg P, Vesström E-L, Watanabe Y and Långström, B. Imaging of aromatase distribution in rat and rhesus monkey brains with [^{11}C]vorozole. *Nuclear Medicine and Biology* 2006; 33: 599-605.

II Takahashi K, Hallberg M, Magnusson K, Nyberg F, Watanabe Y, Långström B and Bergström M. Increase in [^{11}C]vorozole binding to aromatase in the hypothalamus in rats treated with anabolic androgenic steroids. *NeuroReport* 2007; 18: 171-174.

III Takahashi K, Tamura Y, Watanabe Y, Långström B and Bergström M. Alteration in [^{11}C]vorozole binding to aromatase in neuronal cells of rat brain induced by anabolic androgenic steroids and flutamide. *NeuroReport* 2008; 19: 431-435.

IV Takahashi K, Onoe K, Doi H, Nagata H, Yamagishi G, Hosoya T, Tamura Y, Wada Y, Yamanaka H, Yokoyama C, Mizuma H, Takashima T, Bergström M, Onoe H, Långström B and Watanabe Y. Increase in hypothalamic [^{11}C]vorozole binding to aromatase in macaque monkeys treated with anabolic androgenic steroids: A PET study. *Manuscript.*

V Hall H, Takahashi K, Erlandsson M, Estrada S, Bergström-Pettermann E and Långström B. Pharmacological characterization of ^{18}F-labeled vorozole analogues. *Manuscript.*

Reprints were made with permission from the publishers: Elsevier Inc. (I) and Lippincott Williams & Wilkins (II and III).

Related publication

Erlandsson M, Karimi F, Takahashi K and Långström B. ^{18}F-Labelled vorozole analogues as PET tracer for aromatase. *Journal of Labelled Compounds and Radiopharmaceuticals* 2008; 51: 207-212.

Contents

Abbreviations

AAS	Anabolic-androgenic steroids
AR	Androgen receptor
BBB	Blood-brain barrier
BP	Binding potential
BST	Bed nucleus of the stria terminalis
CNS	Central nervous system
DHT	Dihydrotestosterone
DV	Distribution volume
DVR	Distribution volume ratio
ER	Estrogen receptor
FDG	Fluorodeoxyglucose
[^{18}F]FVOO	6-[(*S*)-(4-chlorophenyl)(1*H*-1,2,4-triazol-1-yl)methyl]-1-[2-(2-[^{18}F]fluoroethoxy)ethyl]-1*H*-benzotriazole
[^{18}F]FVOZ	6-[(*S*)-(4-chlorophenyl)(1*H*-1,2,4-triazol-1-yl)methyl]-1-(2-[^{18}F]fluoroethyl)-1*H*-benzotriazole
IC_{50}	Half-maximal inhibitory concentration
K_D	Dissociation constant
LNIM	Logan non-invasive model
MA	Medial amygdala
MPO	Medial preoptic area
OCTX	Occipital cortex
PET	Positron emission tomography
PFCTX	Prefrontal cortex
ROI	Region of interest
SUV	Standardized uptake value
TAC	Time-activity curve
TCTX	Temporal cortex
VOZ	[^{11}C]Vorozole

Introduction

Sex steroids are attracting the attention of researchers not only because of their traditional function [*e.g.*, sexual differentiation in the central nervous system (CNS) and the gonadal glands] but also due to their involvement in neural differentiation and protection and in emotion or mood disorders. Attempts to elucidate the biochemical basis for the gender difference in mood and emotion and in the extreme end of depression and schizophrenia has promoted extensive evaluation of the sex steroid pathways, from synthesis to action on their receptors and modulatory effects on neurotransmitter systems.

Studies on the effects of sex steroids on the CNS started in the 1940's and 50's. Sex steroids were suggested to participate in the induction of differentiation or organization of the CNS during a critical period of development [1]. Studies with dihydrotestosterone (DHT), a non-aromatizable androgen, revealed that part of the actions of sex steroids was achieved by conversion of androgens to estrogens, i.e. aromatization. In 1971, Naftolin *et al.* provided direct evidence of aromatization in the CNS [2,3]. Thereafter several researchers explored the involvement of aromatase in neural cell differentiation, reproductive functions and sexual behavior.

More recently, sex steroids have attracted attention from the viewpoint of emotion. For instance, estrogen has been shown to protect against depression and to delay the onset of schizophrenia and Alzheimer's disease, and estradiol increased the expression of genes for the 5-hydroxytryptamine 5-HT_{2A} receptor [4]. For a long time we have been interested in the development and application of imaging tools that could support an understanding of specific aspects of brain biochemistry and physiology; and in this sense neurosteroids and their role in normal and disease has been one such target. The option to monitor aromatase in the brain of living matter and its protein expression in relation to gender, emotional status and drug abuse warranted our attention.

In 1998, our laboratory developed a positron emission tomography (PET) tracer for aromatase, VOZ [5]. At that time the whole-body distribution of VOZ was investigated in living rhesus monkey, and the potential of this tracer to visualize aromatase in granulosa cells of the ovary was covered; however, the dynamics of the tracer in the living brain was not evaluated.

This thesis aims to qualify the aromatase imaging technique *in vitro* and *in vivo*, and to apply the technique for investigation of brain aromatase under conditions simulating abuse by anabolic steroids.

Aromatase

Sex steroids are formed during the metabolism of cholesterol (Figure 1). At the downstream end of this metabolism, estrogens are generated from androgens by the enzyme, known as aromatase.

The aromatase enzyme complex is composed of a specific aromatase cytochrome P450, the product of the CYP19 gene, and the flavoprotein NADPH-cytochrome P450 reductase [1]. Aromatase cDNA clones encoding human placental [6], monkey [7], rat [8,9], mouse [10], chicken [11], quail [12], zebra finch [13], bovine [14], rainbow trout [15] and channel catfish [16] aromatase enzymes have been isolated and characterized. Among these ten species a high degree of sequence homology is observed (especially in the heme domain), thus suggesting the importance of aromatase in development and function over evolutionary time. In the human placenta, monkey brain, mouse ovary, zebra finch ovary, and rat ovary, there are two or three species of mRNA; however, the smaller aromatase mRNA dose not code for the heme domain (or the substrate binding pocket) and instead contain an unspliced intron. This fact suggests that the latter transcripts cannot encode a functional aromatase enzyme. Aromatization, the conversion of androgens to estrogens, takes place in the endoplasmic reticulum of the cell and is classified as a mixed-function oxidase reaction.

The binding site for the substrate is a highly conserved heme domain of the protein [17,18] and is involved in catalyzing the aromatase reaction. Aromatase has the same single binding site for the different substrates and inhibitors, which site is located at the I-helix and C-terminus of the enzyme [19].

In humans, aromatase is found in several different tissues: placenta, granulosa cells in the ovary, adipose tissue, skin fibroblasts, CNS, hair follicles, Leydig cells in the testicle, liver and muscle. Brain aromatase has been detected in many mammalian species (e.g., human, monkey, rat, mouse, guinea pig, hamster, rabbit and ferret) as well as in other vertebrate species [1]; however, the distribution and activity of aromatase in mammals has been mainly studied in rodents.

The distribution of aromatase in the brain has been examined in several species at multiple levels, including enzyme activity and protein and mRNA expression. Highly localized expression of aromatase is observed in hypothalamic and limbic regions. The highest aromatase activity is found in the amygdala and bed nucleus of the stria terminalis (BST) and moderate levels are detected in the preoptic area [7,20-23]. Other brain regions such as the hippocampus, various regions of the cerebral cortex, midbrain, sensory afferent neurons, and spinal cord also contain aromatase activity and immuno-

reactivity, implying local formation of estrogens possibly related to other neural functions, *e.g.*, cognition, memory, and sensory perception [24-28]. Under normal conditions aromatase is expressed in neurons, though it can also be expressed in astrocytes under some particular conditions, *e.g.*, brain injury [29]. This expression implicates local estrogen formation by astrocytes in brain repair, since estrogens are known to have neuroprotective function [30-32].

The developmental profile of brain aromatase has been mainly investigated in rats and mice. In the rat, the highest levels of brain aromatase are demonstrated during prenatal development. Aromatase activity in the hypothalamus of both sexes begins to increase drastically after gestational day 16 and reaches a peak at gestational day 19, then declines to low levels on the expected day of birth [33-36]. The aromatase levels in the hypothalamus of the mouse display a pattern similar to that in the rat [37-39]. Aromatase activity remains at low but detectable levels for the remainder of life. In adults, males show slightly to moderately higher aromatase activity levels than females [33-35,40-42]

Aromatase deficiency may lead to a range of symptoms and disorders. Aromatase knock out mice show apoptosis of dopaminergic neurons in the medial preoptic area (MPO), reduced thymus mass, hepatic steatosis, insulin resistance, reduced femur length, infertility [43] and loss of aggressive behavior [44]. The clinical phenotype of an aromatase-deficient male human comprises tall stature, a history of persistent linear growth, unfused ephiphyseal cartilages, delayed bone age, osteopenia/osteoporosis, eunuchoid proportion of the skeleton, and progressive worsening of the bilateral *genu valgum* [45] Aromatase-deficient humans display impaired glucose metabolism and insulin resistance [46-49], lipid metabolism disorders, liver function impairment [43] and a variable degree of alteration in fertility [50].

Estrogens and mood

Estrogens have been supposed to affect mood since women are more vulnerable than men to develop depression disorders or anxiety. Women are twice as likely to experience major depression, particularly unipolar depression compared to men [51-53]. Most types of anxiety disorders (*i.e.*, social anxiety, phobias, post-traumatic stress disorder, general anxiety disorder) are more common among women than men [54-57]. Transdermal administration of estradiol decreased self-reported negative mood in women with severe premenstrual syndrome [58].

Removal of ovaries, the primary source of estradiol, increases anxiety and depression behavior and subcutaneous administration of estradiol reversed these effects in rat [59-61]. The estradiol level declines in the postpartum state, and withdrawal from chronically sustained estradiol levels in ovariec-

tomized rats increases depressive behavior [62]. These data suggest that reduced estradiol levels can cause anxiety and depressant-like behavior.

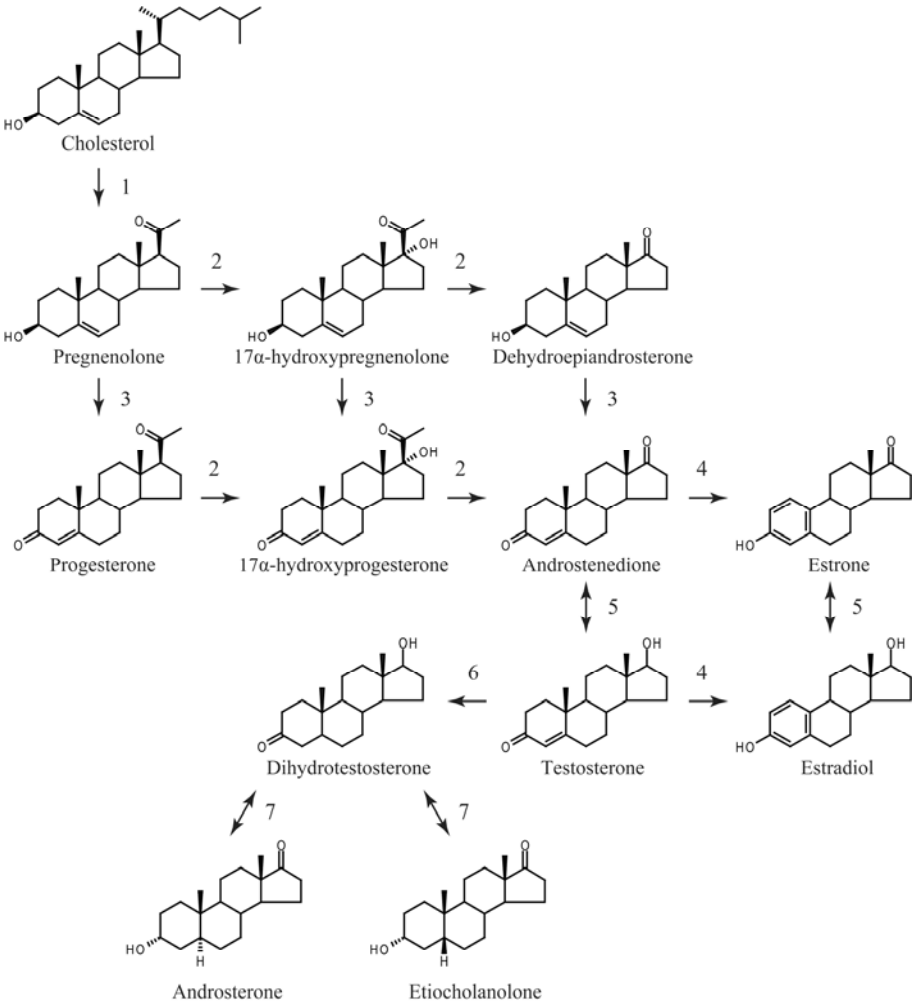

Figure 1. The pathway for steroidogenesis. 1: P450scc cholesterol side-chain cleavage enzyme, 2: P450 17α-hydroxylase, 3: 3β-hydroxy steroid dehydrogenase, 4: aromatase, 5: 17-hydroxysteroid dehydrogenase, 6: 5α-reductase (5β-reductase), 7: 3α-hydroxylase.

Positron emission tomography (PET)

Principle of PET

PET is one of the molecular imaging techniques that enable the observation of regional kinetics of labeled molecules, including their interaction with specific proteins in living beings. A compound that is labeled with a positron-emitting radionuclide (*e.g.*, ^{11}C, ^{18}F or ^{15}O), referred to as a tracer, is injected into the living body, circulates throughout the vascular system, and then reaches and binds to a target molecule. Throughout this process, the radioactive nucleus decays by emission of a positron that within about 1 mm meets an electron, at which time annihilation occurs. In this annihilation, two photons are simultaneously emitted in opposite directions (γ-rays). These gamma rays are recorded by detectors in the PET camera in coincidence (simultaneously) and stored in a computer with respect to position in space. After the end of the acquisition, PET images are reconstructed (Figure 2) either as static images (integrated to one time point) or as dynamic imaging sequences. The latter allow an analysis of the kinetic behavior of the radiotracer for any selected anatomical region, and allow together with plasma tracer kinetics an estimate of specific parameters governing this kinetics, such as binding and interaction with the target. The PET technique has a high sensitivity and high accuracy; and therefore, labeled compounds allow highly quantitative evaluations with a very little amount of mass. Furthermore, positron-emitting nuclides are short lived (*e.g.*, ^{11}C, half-life 20 min; ^{18}F, 110 min); hence radiation exposure is moderate, consequently enabling the observation of physiological or biochemical changes with minimal risk or effect on the subject.

The same labeled tracers using either the β^+ or the 511-keV annihilation photons can be used in *in vitro* experiments allowing pre-clinical qualifications to the aimed tasks prior to translation to humans.

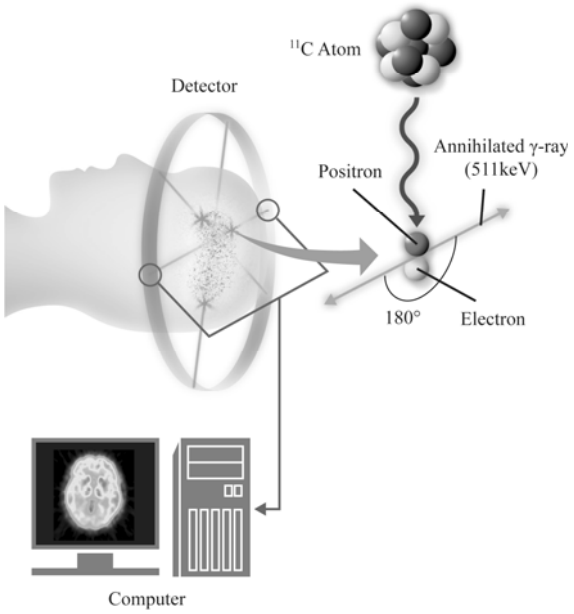

Figure 2. The principle of detecting positron emission with the PET camera.

Application of PET

The predominant clinical use of PET is for cancer diagnosis. Active tumor cells have a high utilization of glucose for their accelerated functions including proliferation; and, therefore, these cells take up a glucose analog, fluorodeoxyglucose (FDG) labeled with the positron-emitting nuclide, ^{18}F. The focal high accumulation of FDG is readily seen in the PET image, making it a sensitive method to diagnose cancer. Other radiolabeled compounds are also available for diagnosis, e.g., ^{15}O-labeled H_2O to monitor cerebral blood flow, ^{11}C-labeled raclopride to demonstrate the distribution of dopamine D_2 receptors [63], ^{11}C-labeled Pittsburgh Compound-B (PIB) to display amyloid-β in Alzheimer's disease [64], *etc*. The central theme of this thesis work is the imaging of an enzyme (aromatase). In our laboratory, ^{11}C-labeled novel tracers for several enzymes have been developed. Studies on monoamine oxidase-B using the ^{11}C-labeled-irreversible L-deprenyl was the first example [65]; and ^{11}C-labeled harmine, a tracer for monoamine oxidase-A, was later developed and used to image brain MAO-A [66]. PET studies were performed with this tracer in neuroendocrine gastroenteropancreatic cancer patients, and the results revealed that ^{11}C-labeled harmine could visualize tumors [67]. Another tracer, ^{11}C-labeled metomidate, was also produced in our laboratory [68]. Metomidate is an analog of etomidate, which is an in-

hibitor of 11β-hydroxylase [69,70]; and it inhibits the synthesis of cortisol and aldosterone in the adrenal cortex. ^{11}C-Labeled metomidate succeeded to visualize adrenal cortical tumors [71].

The PET technique is becoming an important tool in drug development. The distribution in humans to confirm access to a target organ, *e.g.*, the brain, can be made at a very early stage in a drug's development through the new concept of PET microdosing [72]. Human subjects are administered short-lived radiolabeled drug candidates in microgram amounts to describe the drug's concentration-time profile in body tissues targeted for treatment. An important application is the evaluation of the degree of receptor or enzyme occupancy as recorded with PET to ensure adequate dosing and dosing regime. The native target expression is evaluated with PET before drug administration, and after drug administration the degree of reduction in target availability is evaluated in repeat studies.

PET as a research tool in neuroscience

The brain is a complicated organ, and the difficulties to study it are increased by its inaccessibility; thus, only postmortem studies are possible for elucidation of the biochemistry of the human brain. A technique that enables the investigation of biochemistry and physiology in the living brain non-invasively is therefore highly warranted. Typical novel brain-imaging techniques include PET, functional magnetic resonance imaging (fMRI), and near-infrared spectroscopy (NIRS). A characteristic use of PET as a tool in neuroscience is the visualization of neurotransmitters and their receptors and proteins involved in neurodegenerative diseases. In our laboratory, ^{11}C-labeled 5-hydroxytryptophan and L-DOPA were developed for brain imaging [73]. These tracers allow the *in vivo* measurement of neurotransmitter synthesis rate, *i.e.*, formation of dopamine and serotonin, respectively. ^{11}C-Labeled 5-hydroxytryptophan was also taken up in endocrine tumors [74] and this tracer revealed the inverse associations between worsening of cardinal symptoms of premenstrual dysphoria and serotonin formation [75]. ^{11}C-Labeled L-DOPA can be used to evaluate the effect of therapeutic L-DOPA on Parkinson's disease [76].

To investigate the sex steroids system, there are a few tracers available. For visualization of estrogen receptors (ERs), ^{11}C-labeled 17α-methylestradiol [77], ^{11}C-labeled tamoxifen [78], ^{18}F-fluoroestradiol [79], ^{18}F-16α-fluoroestradiol-3-sulphamate [80], *etc*. can be used. Androgen receptors (ARs) can be visualized with ^{18}F-labeled 7α-fluoro-17α-methyl-5α-DHT [81], ^{18}F-labeled 20-fluoromibolerone [82], ^{18}F-labeled 16β-fluoro-7α-methyl-19-nortestosterone, *etc*. However, hitherto these tracers have found application predominantly in oncology for tumors outside the brain.

PET radionuclides

The most commonly used PET radionuclides are ^{11}C, ^{13}N, ^{15}O, and ^{18}F. The most prominent character of these radionuclides is a very short half life, *i.e.*, approximately 20, 10, 2, and 110 min for ^{11}C, ^{13}N, ^{15}O, and ^{18}F, respectively. ^{11}C, ^{13}N and ^{15}O allow repetitive scans during the same day. ^{18}F has a longer half life compared to the others, which makes distribution possible. Therefore, facilities without a cyclotron can perform PET scans with ^{18}F-labeled compounds delivered from outside.

One important feature of PET tracers is their high specific radioactivity, which indicates the amount of radioactivity per unit mass. With higher specific radioactivity, good signals at a very low mass concentration can be obtained, allowing true tracer studies where no pharmacological effect of the mass is generated. The injected tracer dose in a PET study is very low.
Another important factor is that with ^{11}C a very large range of organic molecules can be labeled, hence giving great opportunities for the development of specific probes for different research questions.

Aromatase inhibitors

Clinical purpose

Nowadays the administration of aromatase inhibitors is one of the golden standards for the treatment for estrogen-dependent breast cancer. Estrogen-dependent tumor cells have ERs, and estrogen promotes tumor cell proliferation. To suppress the proliferation of estrogen-dependent tumor cells, there are two types of hormone treatment, *i.e.*, anti-estrogen treatment and aromatase inhibitor treatment.

For anti-estrogen treatment, mainly tamoxifen is used. Tamoxifen is a selective ER modulator and functions as an antagonist in breast tissue [83]. When a tumor becomes tamoxifen resistant, an aromatase inhibitor becomes the second choice (there are also cases in whch aromatase inhibitor is the first choice). Aromatase inhibitors prevent the conversion of androgens to estrogens, consequently reducing the production of estrogens. This inhibition occurs predominantly in the ovary in pre-menopausal women and in fat in post-menopausal women, but inhibition of the local estrogen production in tumor stroma cells may also be important. If estrogens, which bind to ER of breast tumor cells, are reduced in amount, the estrogen drive of proliferation of tumor cells is thus interrupted.

Types of aromatase inhibitors

Aromatase inhibitors can be divided into two categories, namely steroidal inhibitors and non-steroidal inhibitors. Steroidal inhibitors have structural similarity to endogenous androgens.

Vorozole was developed as a specific non-steroidal aromatase inhibitor for breast cancer treatment [84-87]; however, it was withdrawn from testing when no difference was detected in the duration of median survival as compared with the progestational agent megestrol acetate. Vorozole is a triazole derivative, which includes anastrozole (Arimidex™) [88] and letrozole (Femara™) [89,90]. These triazole derivatives have good specificity and selectivity for aromatase. Vorozole binds reversibly to aromatase and has an 8-hour half life in plasma. The IC_{50}-value of vorozole is 1.4 nM [87] and the clinical dose for humans is 2.5 mg once daily [91]. No effect on P450-dependent cholesterol synthesis, cholesterol side-chain cleavage and 7α-hydroxylation and 21-hydroxylase [85] and no estrogenic or antiestrogenic property were detected *in vitro* or *in vivo* [84].

Anabolic-androgenic steroids

Anabolic-androgenic steroids (AAS) are testosterone derivatives that are used either clinically or by athletes for their anabolic properties. AAS is used medically for treatment of anemia, osteoporosis, hypogonadism, and more recently, for HIV wasting syndrome.

The abuse of AAS has become a major drug problem over recent decades, not only with athletes and bodybuilders wishing to enhance their performance, but also for the broader population, including adolescent males not necessarily connected to sports. Such adolescent males administer AAS not only to improve their appearance and enhance muscular mass, but also to increase self-esteem and to acquire an improved fighting skill [92]. AAS are also administered for intoxication. Up to 4% of high school students in North America are estimated to have used AAS [93]. In the course of AAS abuse, it has also become clear that it leads to mood swings (positive and negative), extreme aggressive behavior, and unprovoked rage attacks, as well as anxiety and depression. The behavioral changes in humans have been confirmed in rats treated with nandrolone, which display an aggressive behavior when tested in a defensive aggression model [94]. This aggression is also associated with neurochemical changes in the brain. Changes in the expression of c-Fos, serotonin receptors, and the glutamate system have been reported [95,96]. These changes might all relate to the observed increased aggression in rats and in humans. Furthermore, chronic treatment with nandrolone has been shown to elevate the levels of substance P in regions asso-

ciated with aggression such as the amygdala, hypothalamus, and periaqueductal gray in rats [97].

In the present thesis work, nandrolone decanoate was employed as an AAS. Nandrolone decanoate is a prodrug of nandrolone, which has a similar chemical structure as endogenous androgen, testosterone (Figure 3) and has higher affinity for the AR and is more potent than testosterone.

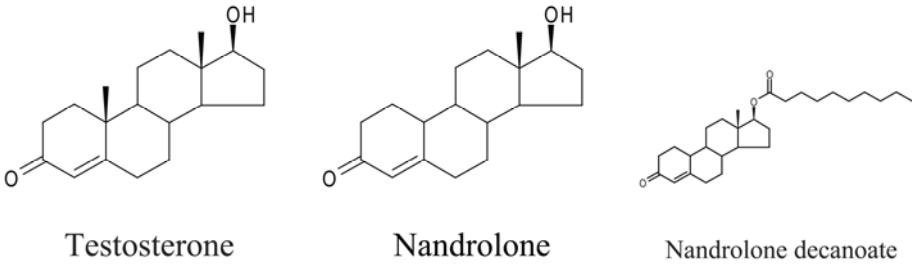

Testosterone Nandrolone Nandrolone decanoate

Figure 3. Chemical structures of the endogenous androgen testosterone; its synthetic derivative, nandrolone; and the prodrug, nandrolone decanoate.

Aim of the thesis

The aim of this thesis was to explore and qualify radiolabeled vorozole for imaging of aromatase in the brain by using PET.

The specific aims were the following:

- To demonstrate a regional pattern of specific VOZ binding in *in vitro* and *in vivo* experiments that correlates with the known distribution of aromatase;
- To investigate the effect of AAS on brain aromatase;
- To explore new tracers with potential better or different characteristics for visualization of brain aromatase.

Materials and Methods

Animals and treatment

Male and female Spraque-Dawley rats (average weight, 260 g) and male and female rhesus monkeys were used. All animals were handled according to the guidelines by the Swedish Animal Welfare Agency.

In Paper II, male rats were divided into two groups: control and nandrolone-treated groups. Nandrolone-treated rats received one daily intramuscular injection of nandrolone decanoate at a dose of 15 mg/kg body weight. The control group received sterile peanut oil. Injections were administered for 14 days. The animals were decapitated on day 15, and the brains were rapidly removed and stored at -80 ˚C for autoradiography.

In Paper III, male rats were divided into four groups: control, nandrolone, flutamide (anti androgen), and nandrolone plus flutamide treatment groups. Nandrolone-treated rats and nandrolone-plus-flutamide-treated rats were injected with nandrolone decanoate (15 mg/kg, once every 3 days). Flutamide-treated rats and nandrolone-plus-flutamide treated rats received daily flutamide (20 mg/kg) intraperitoneally. The treatment lasted for 20 days. The rats were then sacrificed in a high concentration of CO_2, and their brains were rapidly removed and stored at -80 ˚C for autoradiography.

Four female rhesus monkeys (*Macaca mulatta*; Paper I), four male rhesus monkeys (Paper IV), and one female rhesus monkey (Paper V) were used for PET studies. The four male rhesus monkeys were given nandrolone decanoate (6.3 mg/kg) intramuscularly once a day every day for 21 days.

The rats and monkey studies were approved by the local Research Animal Ethics Committee (C266/1, C342/97, C117/4, C255/3, C314/5, C234/5 and MAH18-05).

VOZ

^{11}C-Labeled (*S*)-6-[(4-Chlorophenyl)(1*H*-1,2,4-triazol-1-yl)mehyl]-1-mehyl-1*H*-benzotriazole (VOZ) was synthesized from its *N*-desmethylated derivative via reaction with [^{11}C]methyl iodide in dimethyl sulfoxide [5] (Figure 4). The identity and concentration of VOZ were assessed by high-performance liquid chromatography, in the case of identity with added unlabeled vorozole. All batches used in the experiments had > 95% radiochemical purity, and the

specific radioactivity was 24-103 GBq/μmol for *in vivo* studies. In this thesis work, radiolabeled vorozole was utilized as a PET ligand for aromatase, not to inhibit aromatase activity.

[^{18}F]Vorozole analogs

Two different ^{18}F-labeled vorozole analogs, *i.e.*, 6-[(*S*)-(4-chlorophenyl)(1*H*-1,2,4-triazol-1-yl)methyl]-1-(2-[^{18}F]fluoroethyl)-1*H*-benzotriazole, abbreviated as [^{18}F]FVOZ, and 6-(*S*)-(4-cholorophenyl)(1*H*-1,2,4-triazol-1-yl)methyl]-1-[2-(2-[^{18}F]fluoroethoxy)ethyl]-1*H*-benzotriazole, designated as [^{18}F]FVOO, were synthesized [98] (Figure 4). The radiochemical yields were in the range of 9-13% after a total synthesis time of 110-120 min, and the specific radioactivities were 175 GBq/μmol and 56 GBq/μmol, respectively.

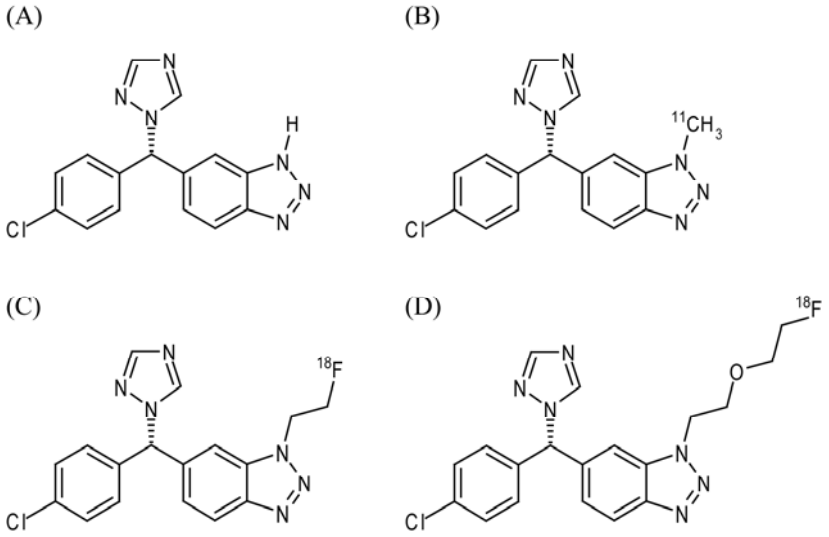

Figure 4. Chemical structures of *N*-desmethylated vorozole (precursor, A), VOZ (B), [^{18}F]FVOZ (C), and [^{18}F]FVOO (D).

Analysis of radiolabeled metabolites in plasma

In Paper I, the metabolite analysis of VOZ in plasma was performed in a monkey at 10, 20, and 45 min after administration of VOZ. The plasma was obtained by centrifugation of the venous blood; and to a 1.2-ml plasma aliquot, 1.2 ml of acetonitrile was added to precipitate the proteins. The ace-

tonitrile contained unlabeled authentic vorozole as a standard. The resulting mixture was centrifuged, and the supernatant was filtered through a 0.2-μm pore-size membrane by centrifugation. The samples were then analyzed by HPLC to separate VOZ from radioactive metabolites. The sample was injected into a column, and the tracer and its metabolites were eluted with acetonitrile-50 mM ammonium acetate. The eluate from the column was collected in three fractions; and VOZ was eluted in the last fraction, as confirmed by observation of the UV peak of the unlabeled standard as well as VOZ by a radio detector. The radioactivity of different fractions was measured in a γ-counter. Consequently, the amount of radioactivity associated with intact VOZ was calculated as a percentage of the total amount of radioactivity.

In Paper IV, the plasma was obtained by centrifugation of the arterial blood. To a 0.2-ml plasma aliquot, 0.2 ml of acetonitrile was added to precipitate the proteins. The resulting mixture was centrifuged, and the supernatant was analyzed for radioactive components by using HPLC with a coupled NaI(Tl) positron detector to measure VOZ and its radioactive metabolites. A fast-gradient condition using two switching pumps was used for the analysis of the samples. The amount of radioactivity associated with intact VOZ was calculated as a percentage of the total amount of radioactivity.

In Paper V, the metabolism of [^{18}F]FVOZ and [^{18}F]FVOO was determined by intravenous injection in a male rat with 50 MBq of the tracers. Blood was collected after 40 min and the presence of metabolites was determined in plasma by using HPLC according to the method developed for VOZ in Paper I.

In vitro autoradiography

Frozen rat brains were sliced into serial coronal sections (25 μm) by using a cryostat microtome, and the sections were thaw-mounted onto glass slides and stored at -20˚C until use.

Consecutive sections were preincubated at room temperature (*ca.* 22˚C) for 10 min in buffer (50 mM Tris-HCl, pH 7.4), and incubated with 2 nM VOZ, [^{18}F]FVOZ or [^{18}F]FVOO (0.01–0.1 MBq/ml buffer) in the presence or absence of unlabeled vorozole (1 μM) at room temperature for 30 (VOZ) or 50 ([^{18}F]FVOZ and [^{18}F]FVOO) min. The sections were then washed and rapidly dried. Sections and calibration standards were exposed to phosphor imaging plates at room temperature for 40 min (VOZ) or >4 hrs ([^{18}F]FVOZ and [^{18}F]FVOO) to generate the autoradiograms. The phosphor plates were scanned and the images were analyzed. Regions of interest (ROIs) were delineated for the BST, medial preoptic area (MPO), and medial amygdala (MA). The signal of equivalent slices incubated with unlabeled vorozole was determined as nonspecific binding, and specific binding was obtained by

subtraction of nonspecific binding from total binding. The specific binding of each ROI in drug-treated and control groups was normalized by the mean value of all ROIs of equivalent regions in control rats (Papers II and III).

Ex vivo autoradiography

Male rats were injected via a tail vein with [^{18}F]FVOZ or [^{18}F]FVOO (20 MBq/rat in 500 µl). Four rats receiving [^{18}F]FVOZ also received a high concentration (5 mg/kg i.v.) of unlabeled vorozole. After 50 min the rats were sacrificed, and the brains were dissected out, frozen, and mounted for cryosectioning. Frozen sections (50µm) were prepared in a cryostat microtome and placed on glass slides. Consecutive sections covering the amygdala were taken. The slides were dried and exposed to phosphor imaging plates for >4 hrs. The plates were then scanned.

Organ distribution

Male and female rats were injected intravenously with *ca.* 12 MBq of [^{18}F]FVOZ or [^{18}F]FVOO per animal. The animals were sacrificed after 5 – 240 min, and selected organs were dissected out. Blood, heart, lung, liver, pancreas, spleen, adrenal, kidney, intestine (with and without contents, and large intestine), feces, urinary bladder, ovary or testis, muscle, bone (femur), and brain were collected and weighed; and the radioactivity was measured and corrected for radioactive decay in a γ-counter. Organ values were calculated as standardized uptake value (SUV) as follows:

$$SUV = \frac{Radioactivity\ in\ organ / Weight\ of\ organ}{Injected\ radioactivity / Body\ weight}$$

Binding assays

VOZ (Paper I)

Male rats were sacrificed by an ascending atmospheric concentration of CO_2, their brains were rapidly removed, and a pair of the amygdala was dissected on ice and homogenized in 1 ml of 0.32 M sucrose solution.

For association experiments, duplicates of homogenate tissue were incubated with 2 nM VOZ at room temperature. Binding was started at different time points (2, 5, 10, 25, 40, and 60 min) in reverse order and terminated

simultaneously in all samples at Time 0 by filtration through glass fiber filters that had been previously soaked in 0.3% polyethylenimine for 1 h, followed by three washes with 2 ml of buffer by using a cell harvester system. Filters were placed in vials for counting in a γ-counter.

For ligand saturation experiments, duplicates of homogenate tissue were incubated with ascending concentrations of VOZ (0.1, 0.3, 0.7, 1.0, 3.0, and 5.0 nM) at room temperature for 30 min. Nonspecific binding was obtained by the incubation of adjacent samples with 1μM unlabeled vorozole. Filtration and counting in a γ-counter were performed. The means of K_D and B_{max} were calculated by Scatchard plot analysis.

[^{18}F]FVOZ and [^{18}F]FVOO (Paper V)

Female rats were sacrificed by an ascending atomospheric concentration of CO_2. The ovaries were dissected, weighed, and homogenized in 10 volumes of ice-cold 0.3 M sucrose. The crude homogenate was aliquoted, immediately frozen in EtOH/CO_2 and stored at -80˚C until used. Homogenates were thawed and 100-μl aliquots (for [^{18}F]FVOO) or 20-μl aliquots (for [^{18}F]FVOZ) were incubated with the radioligands at final concentrations of 0.001, 0.003, 0.01, 0.03, and 0.1 MBq/ml in PBS, pH 7.4, at room temperature for 60 min. Nonspecific binding was defined as residual binding in the presence of 1 μM unlabeled vorozole. Triplicate samples were used. Filtration and counting in a γ-counter were performed. Saturation curves were generated, and K_D and B_{max} were calculated.

Immunohistochemistry

Rats were deeply anesthetized with diethyl ether and perfused via the heart with 4% formaldehyde buffered with 0.1 M phosphate-buffered saline (PBS, pH 7.4). The brains were removed, post-fixed in 4% formaldehyde buffered with 0.1 M PBS overnight at 4˚C, and then immersed in 30% sucrose solution. Serial brain sections (30 μm) were prepared with a cryostat and collected as free-floating sections. For immunohistochemical detection of aromatase in relation to neurons, double staining was performed. Brain sections were incubated with monoclonal mouse anti-aromatase antibody (1:100) at 4˚C for 63 h followed by incubation with biotinylated anti-mouse IgG antibody (1:200). Immunohistochemical detection of aromatase was performed using the avidin-biotin-peroxidase complex method with 3,3'-diaminobenzidine (DAB) and nickel sulphate solution. Subsequently, the same sections were incubated with monoclonal mouse anti-neuronal nuclei antibody (NeuN, 1:500) at 4˚C for 17 h and then incubated with biotinylated anti-mouse IgG antibody. Immunohistochemical detection of neurons was performed using the avidin-biotin-peroxidase complex method with DAB.

PET studies in rhesus monkeys

In Paper I, the female monkeys were anesthetized with propofol (10 mg/kg/h) after ketamine induction. Tracrium was given at 0.5 mg/kg/h. The monkeys were intubated and maintained with sevoflurane inhalation anesthesia and artificial ventilation. Before emission scans, transmission scans were performed for 10 min and used for attenuation correction. VOZ was administered intravenously as a bolus. After the baseline scan, unlabeled vorozole was infused (100 μg/kg) for 5 min; and, immediately thereafter, the next VOZ was injected. One scan lasted for 100 min.

In Paper IV, four male monkeys were scanned with PET before and directly after a three-week daily nandrolone treatment, and two of the four male monkeys were scanned again one month after the nandrolone treatment. For the PET scans, the monkeys were sedated with ketamine (10 mg/kg), and then anesthetized with a continuous infusion with propofol (10 mg/kg/h). Transmission scans were performed for 30 min and followed by emission scans carried out for 90 min. VOZ was injected intravenously as a bolus.

In Paper V, one female rhesus monkey was anesthetized with propofol (10 mg/kg/h) after ketamine induction. The monkey was intubated and maintained with sevoflurane inhalation anesthesia and artificial ventilation. [^{18}F]FVOZ (138 MBq) was administered intravenously as a bolus. After 120 min of scanning, unlabeled vorozole was infused (100 μg/kg) during 5 min. The scan was continued for a total of 250 min. Images were reconstructed with attenuation, scatter, and random correction. ROI were delineated in the cerebellum, amygdala, preoptic area, temporal cortex (TCTX) and occipital cortex (OCTX).

Analysis of PET data in rhesus monkey brain

In Paper I, ROIs were delineated in one slice representing the cerebellum, both amygdala, TCTX, and OCTX. For each of these four regions, decay-corrected time-activity curves (TACs) were generated. TACs of the amygdala, TCTX and OCTX were divided by that of the cerebellum to indicate the specific binding kinetics.

In Paper IV, volumes of interest (VOIs) were delineated in the cerebellum, amygdala, hypothalamus, thalamus, prefrontal cortex (PFCTX), TCTX, and OCTX. For each of these regions, decay-corrected TACs were produced. With a simplified reference tissue model (SRTM) [99], k_2 was calculated in the cerebellum for each separate animal; and then the average of all animals was determined as k'_2, to represent the efflux rate constant from regions

without aromatase. The estimated k'_2 value was confirmed by a one-tissue compartment model using actual arterial blood sampling from one monkey. The data were analyzed with a Logan noninvasive model (LNIM) [100], and the results were taken from the regression slope (= Distribution volume ratio (DVR) = k_3/k_4+1). The binding potential (BP, = DVR -1=k3/k4) was calculated, and parametric images of BP was generated based on pixel-wise kinetic modeling using the TAC of the cerebellum as an input function and the group average k'_2.

Results

Selectivity and affinity of VOZ for brain aromatase *in vitro*

Autoradiographic images demonstrated the distribution of VOZ binding in the male rat brain (Figure 5). The distribution pattern of specific binding was similar but the amount of specific binding was different, between the sexes. In males, obvious specific binding was observed in the MA and BST, and weaker signal was detected in the MPO; wheares in females, a clear specific binding was observed only in the MA and a weak signal was detected in the BST. Furthermore, no signal was detected in the MPO. Females had significantly lower VOZ binding in the MA and BST compared to males ($p<0.001$) (Figure 5). Specific binding of VOZ in females was 52% and 24% of males in the MA and BST, respectively.

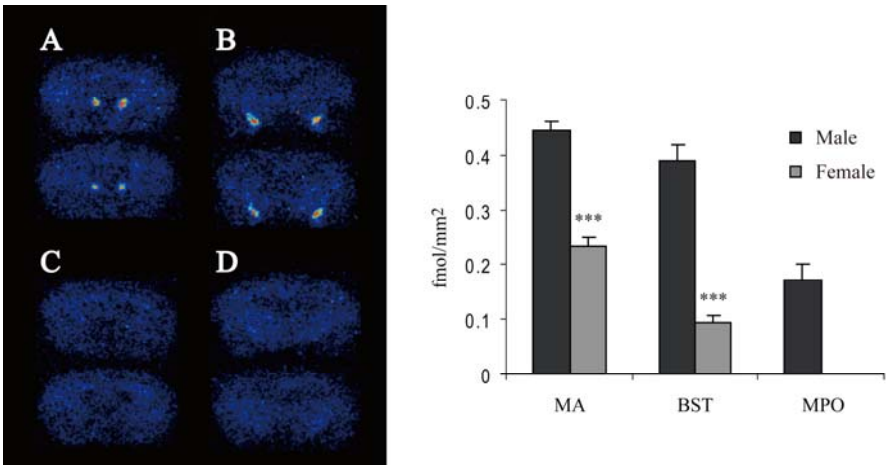

Figure 5. Autoradiographic images (left) and distribution and sex difference (right) of VOZ binding in the rat brain. (A) Total binding in BST; (B) Total binding in MA; (C) Nonspecific binding in BST and (D) nonspecific binding in MA. Nonspecific binding was obtained by co-incubation with unlabeled vorozole. In the MA and BST, females had significantly lower binding than males (***$P<0.001$). The signal of the MPO in females was too weak to be quantified.

With homogenate tissue of the male rat amygdala, the association studies showed that equilibrium was reached within 20 min. The saturation studies indicated a single binding site, as indicated by linearity of the Scatchard plot (Figure 6). The dissociation constant (K_D) of VOZ for aromatase and the B_{max} were determined to be 0.60±0.06 nM and 9.3±1.1 fmol/mg wet tissue, respectively.

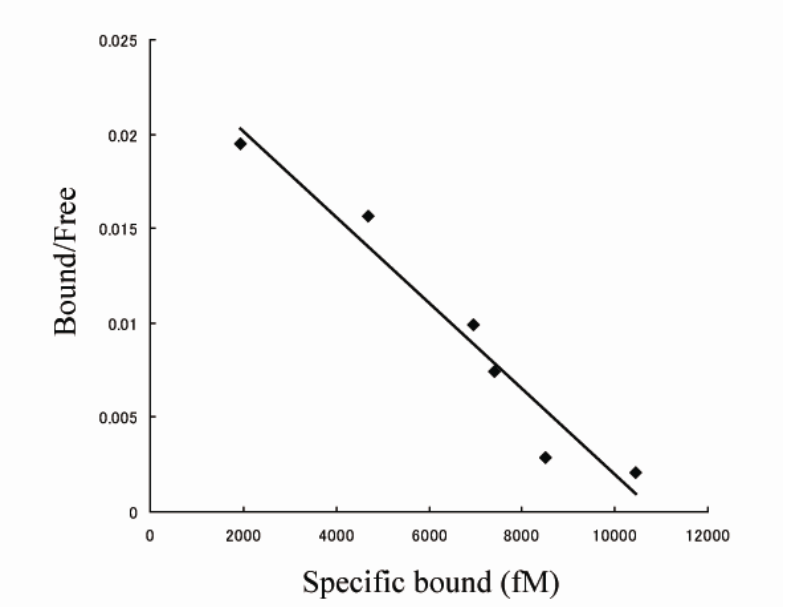

Figure 6. Scatchard plot analysis of specific binding of VOZ. Homogenates from male rat amygdala were incubated with 0.1, 0.3, 0.7, 1.0, 3.0, and 5.0 nM VOZ for 30 min.

In vivo brain aromatase imaging with VOZ

PET images with VOZ in the rhesus monkey brain, with or without a pharmacological dose of vorozole, is presented in Figure 7. A high uptake of VOZ was observed in the amygdala, where the uptake was blocked in the presence of unlabeled vorozole. In two monkeys, an increased signal was observed in the hypothalamus, but in two other monkeys, no such increased signal was observed. The SUV ratio of the amygdala against the cerebellum was higher than that of TCTX or OCTX after 20 min (Figure 8), and the difference in SUV ratio between the amygdala and TCTX at 55 min after the start of scans was 19% ($P<0.001$).

Metabolite analysis of the plasma revealed that 85±0.1%, 77±2%, and 68±4% of vorozole was intact at 10, 20, and 45 min, respectively, after the injection.

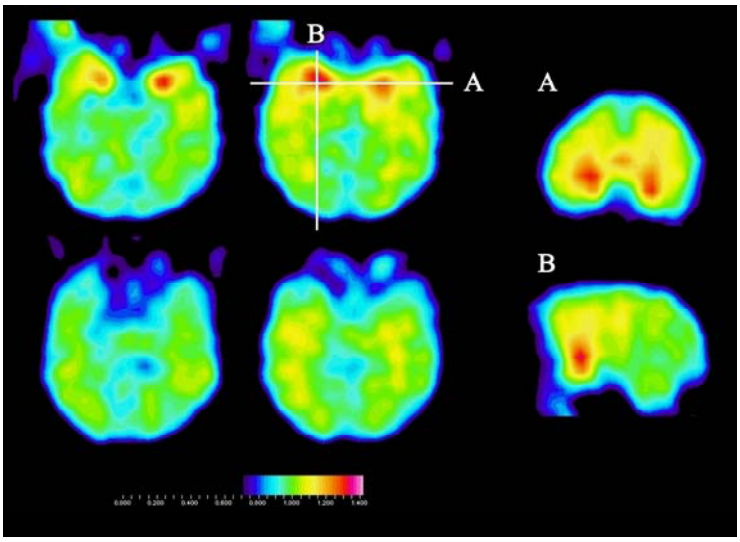

Figure 7. SUV images of a female rhesus monkey brain. The SUV images were normalized to the SUV in the cerebellum. The upper two left PET images illustrate the distribution of VOZ, and the lower two left images show SUV images after the administration of unlabeled vorozole. (A and B) Coronal and sagittal sections at positions indicated in upper right horizontal section.

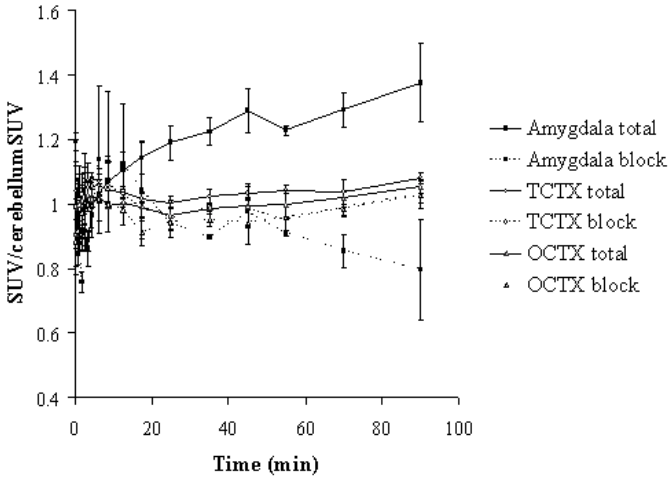

Figure 8. Time-activity curves of VOZ in the amygdala (with or without unlabeled vorozole), TCTX and OCTX normalized by the SUV in the cerbellum.

Alteration in VOZ binding to aromatase in rats treated with nandrolone and flutamide

Paper II: The regions with high specific binding of VOZ did not differ between nandrolone-treated and control rats, namely the BST, MPO, and MA. However, the intensity of the signals was different between the groups in the BST and MPO. The signals of AAS-treated rats were 45 and 81% higher than those of control rats in the BST and MPO, respectively ($P<0.0001$). On the other hand, there was no difference in the MA between the groups (Figure 9).

Paper III: The results of the nandrolone treated group and control group were similar to those presented in Paper II. In addition to those results, flutamide treatment decreased VOZ binding to aromatase in all three regions (control vs. flutamide, MA: 19%, $P<0.01$; BST: 24%, $P<0.01$; MPO: 32%, $P<0.05$; nandrolone vs. nandrolone plus flutamide, MA: 18%, $P<0.01$; BST: 32%, $P<0.0001$; MPO: 33%, $P<0.001$)(Figure 10 and 11). The effects of nandrolone and of flutamide or both on specific binding of VOZ were most pronounced in the MPO.

The immunohistochemical study revealed that the expression of aromatase was increased in neuronal cell bodies of the BST (Figure 12 and 13) and MPO.

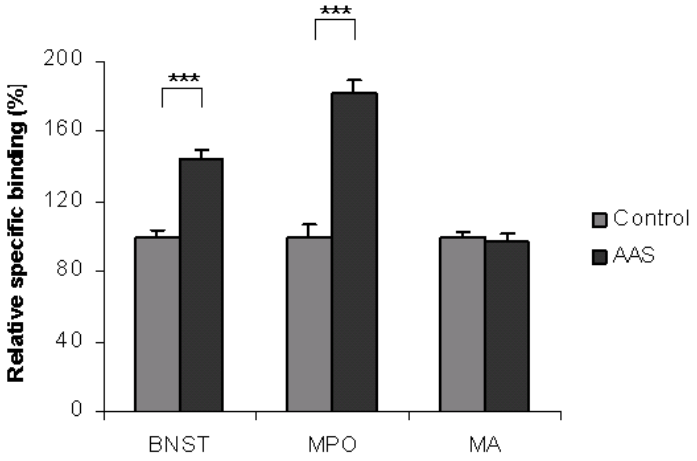

Figure 9. Relative specific binding of VOZ in the BST, MPO, and MA in the AAS (nandrolone)-treated group in comparison with that in the control group.
***P<0.0001.

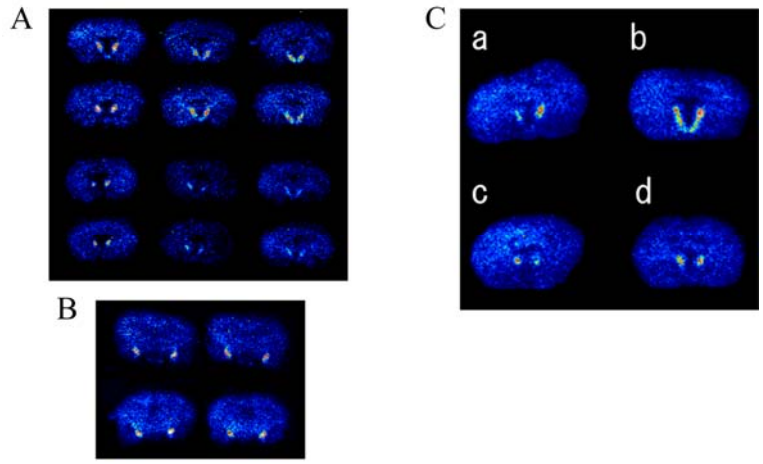

Figure 10. Autoradiograms of VOZ binding to brain aromatase in nandrolone-treated rats (A and B) and nandrolone plus flutamide-treated rats (C). A: BST and MPO of nandrolone-treated rat (**upper six sections**) and control rat (**lower six sections**). B: MA of nandrolone-treated rat (**upper two sections**) and control rat (**lower two sections**). C: rat brain sections including the BST. **a**, control; **b**, nandrolone-treated rat; **c**, flutamide-treated rat; **d**, nandrolone plus flutamide-treated rat.

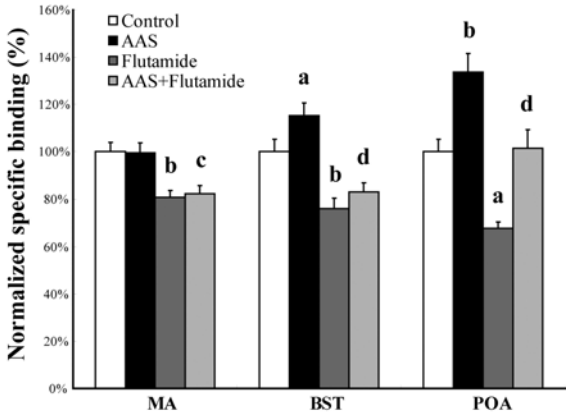

Figure 11. Relative specific binding of VOZ in control, nandrolone-treated rat, flutamide-treated rat, and nandrolone plus flutamide-treated rat. (a, $P<0.05$ vs. control; b, $P<0.01$ vs. control; c, $P<0.01$ vs. nandrolone-treated rat; d, $P<0.001$ vs. nandrolone-treated rat)

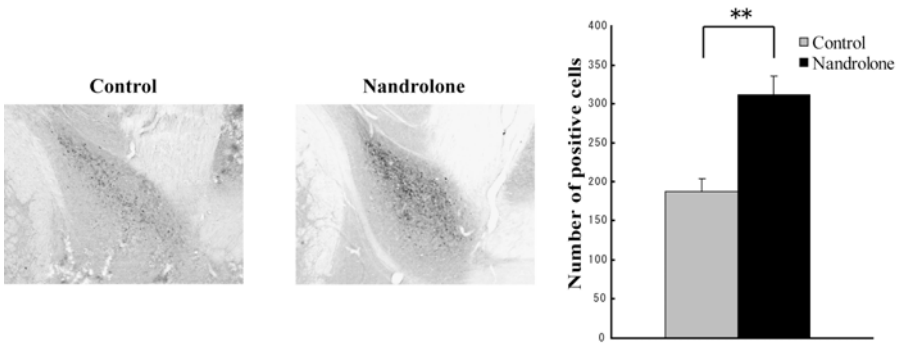

Figure 12. Immunohistochemistry of aromatase-positive cells in the BST. The graph shows the difference in number of these cells in each group. **P<0.01.

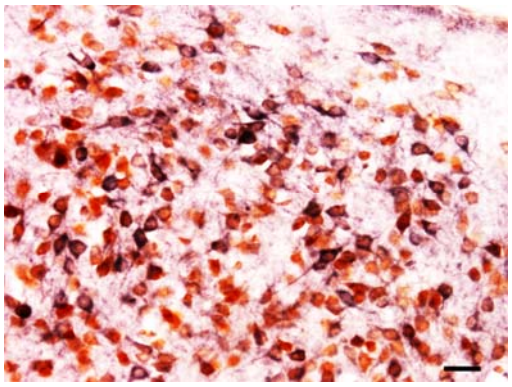

Figure 13. Aromatase expression in neuronal cell bodies of the BST from a nandrolone-treated rat. Aromatase-positive cells (dark blue color) were also positive for neuronal nuclear antigen (orange color). Scale bar=50 μm.

Increase in VOZ binding to aromatase in the hypothalamus in rhesus monkeys treated with AAS

Compared with that under pre-treatment conditions, VOZ binding was increased by 71% in the hypothalamus after a 3-week nandrolone treatment (Figure 14 and 15, P<0.01). On the other hand, the binding in the other specific VOZ-binding region, the amygdala, did not change. The TACs of other cortical regions (PFCTX, TCTX, OCTX) behaved similarly as the TAC of the cerebellum (Figure 16). The BP of two monkeys that had received a PET scan one month after the nandrolone treatment was diverse. The BP in the hypothalamus in one monkey was decreased to the pretreatment level,

whereas in the other monkey the BP in the hypothalamus was increased even more compared with the immediate post-treatment level.

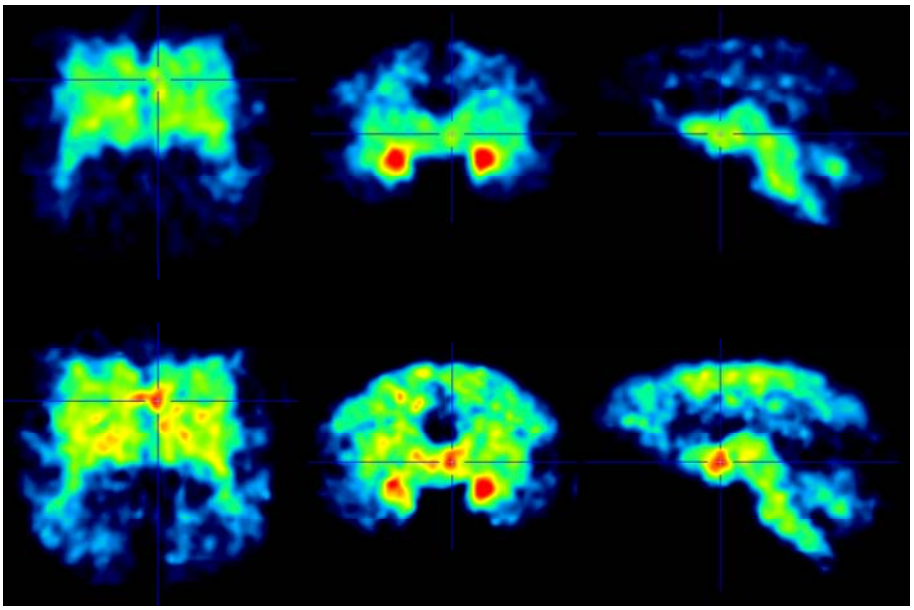

Figure 14. BP images of the pre- and immediate post-treatment rhesus monkey brain. The upper images display pre-treatment BP; and the lower images display post-treatment BP (left images: transaxial, center: coronal, right: sagittal). Cross hairs indicate the hypothalamus. These images suggest that nandrolone treatment increases the VOZ binding in the hypothalamus.

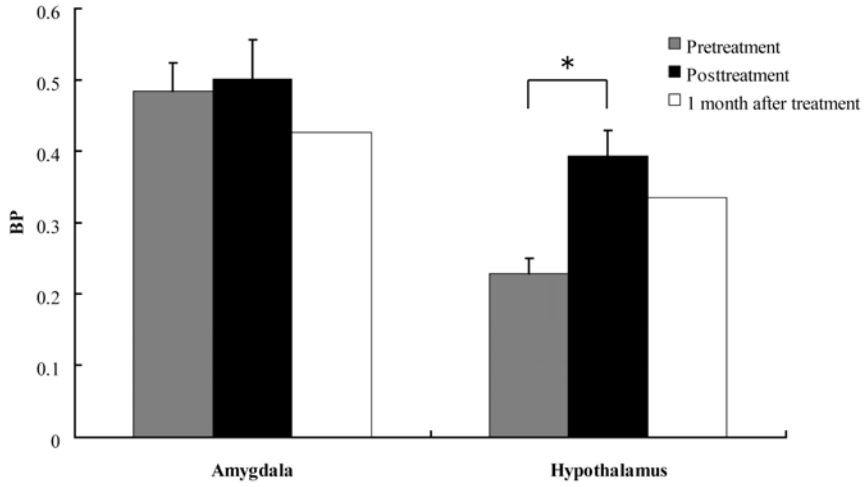

Figure 15. The BP value of pre- immediate post-treatment and one month later in the amygdala and hypothalamus (n=4 in pre- and post-treatment, n=2 at one month later). Paired t-test was performed. *, P<0.05.

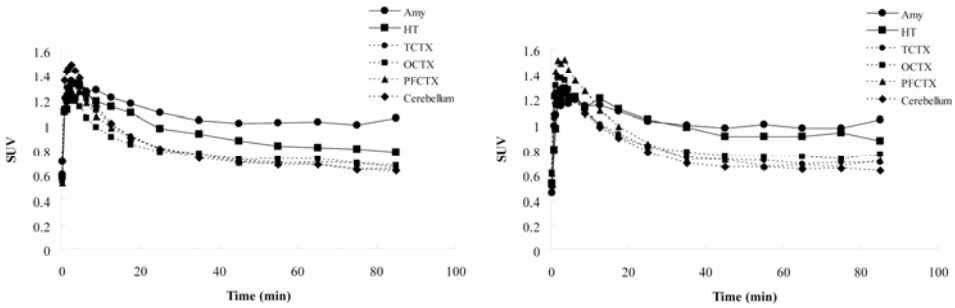

Figure 16. TTAC of VOZ in the amygdala (Amy), hypothalamus (HT), temporal cortex (TCTX), occipital cortex (OCTX), prefrontal cortex (PFCTX) and cerebellum. Left: TAC at pre-treatment, right: TAC immediately post-treatment.

Characterization of ^{18}F-labeled vorozole analogs

In vitro autoradiography

The distribution pattern of [^{18}F]FVOZ and [^{18}F]FVOO binding was similar to that of VOZ binding (Figure 17), *i.e.*, specific binding was observed in the MA, BST and MPO. By adding unlabeled vorozole during incubation, the binding of labeled vorozole analogue in these regions was blocked.

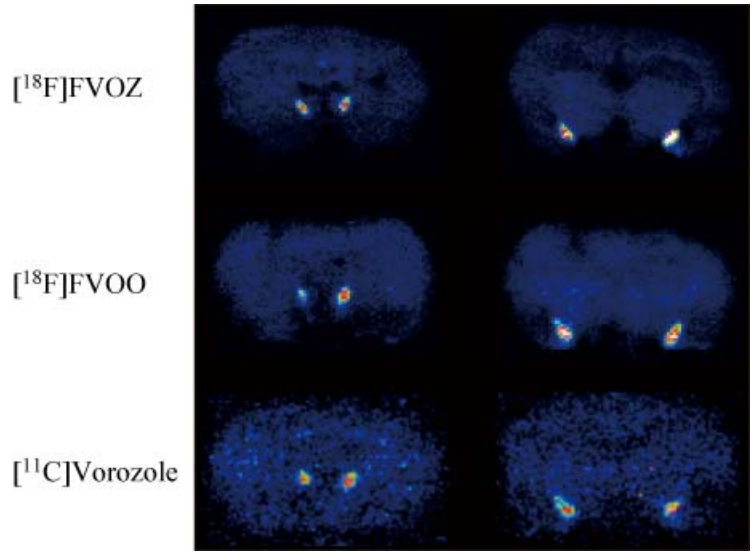

Figure 17. Autoradiographic images of [^{18}F]FVOZ, [^{18}F]FVOO, and VOZ in a male rat brain. The left slices include the BST, and the right ones, the MA.

Ex vivo autoradiography

Male rats were injected with [^{18}F]FVOZ, of which two rats also were given unlabeled vorozole. Specific binding of [^{18}F]FVOZ was observed in the amygdala. No regional binding in the brain could be seen in any male rats injected with [^{18}F]FVOO.

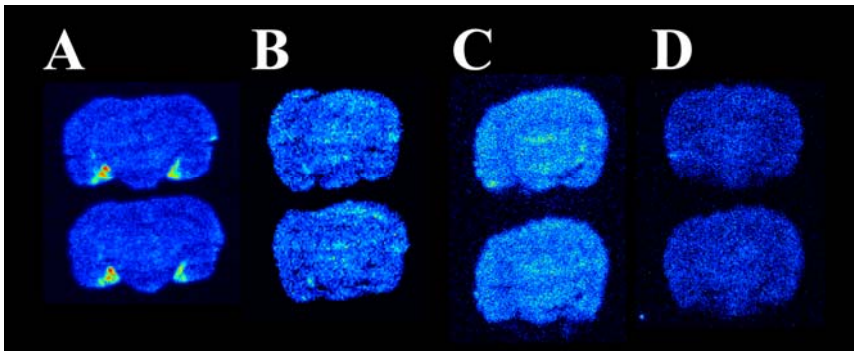

Figure 18. Ex vivo autoradiographic images of [^{18}F]FVOZ and [^{18}F]FVOO. The two slices in each column are consecutive. A: Total binding of [^{18}F]FVOZ, B: Non-specific binding of [^{18}F]FVOZ, C: Total binding of [^{18}F]FVOO, D: Nonspecific binding of [^{18}F]FVOO.

Binding studies using homogenates from ovaries

The radioactivity concentrations used in the assays were converted to molar concentrations by using the specific radioactivity for each batch, and saturation curves were plotted (Figure 19). Calculated values for K_D and B_{max} were 0.21±0.1 nM and 210±20 fmol/mg wet tissue, respectively, for [^{18}F]FVOZ and 7.6±1 nM and 293±12 fmol/mg wet tissue, respectively for [^{18}F]FVOO.

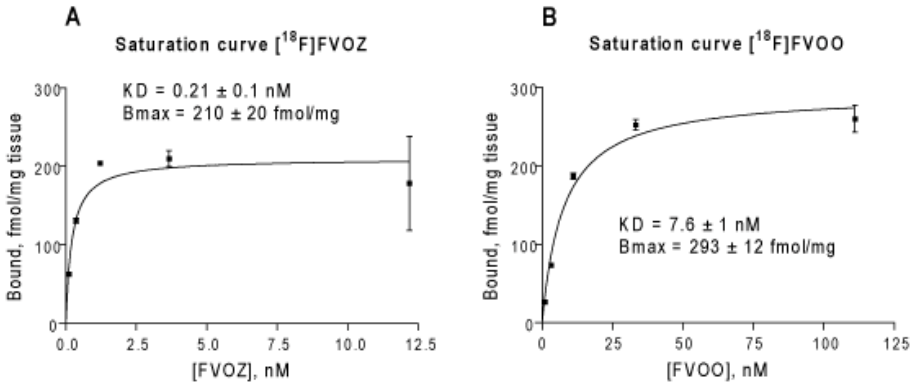

Figure 19. Saturation curves in homogenate from rat ovary of A: [^{18}F]FVOZ and B: [^{18}F]FVOO.

Organ distribution

The distribution of [^{18}F]FVOZ and [^{18}F]FVOO in various male and female rat organs are shown as SUV values in Figure 20. The highest levels were observed in the kidney, adrenal, and liver; but substantial radioactivity was also found in other organs. The time-dependent uptake in bone indicates a slight defluorination of the radioligand. Very low radioactivity was found in brain or cerebellum compared with that in other organs.

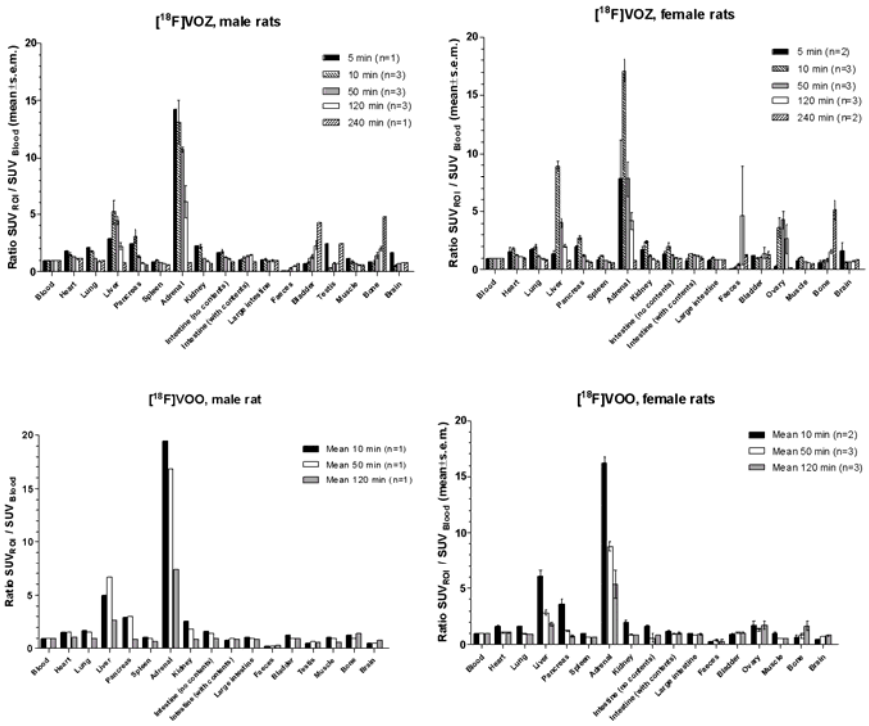

Figure 20. Organ distribution of [^{18}F]FVOZ and [^{18}F]FVOO.

Monkey PET

The monkey PET study showed that [^{18}F]FVOZ accumulated in the amygdala and hypothalamus, with virtually no specific binding in the cortex (Figure 21). The specific binding was displaced by the addition of a high dose of unlabeled vorozole (Figure 22). No monkey PET study with [^{18}F]FVOO was performed because [^{18}F]FVOO was so rapidly metabolized. The metabolite analysis using rats revealed that 30% of [^{18}F]FVOZ and 9% of [^{18}F]FVOO were intact at 40 min after the injection.

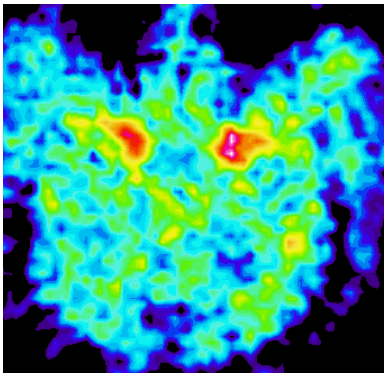

Figure 21. PET image of [^{18}F]FVOZ contained in the amygdala region of a rhesus monkey brain.

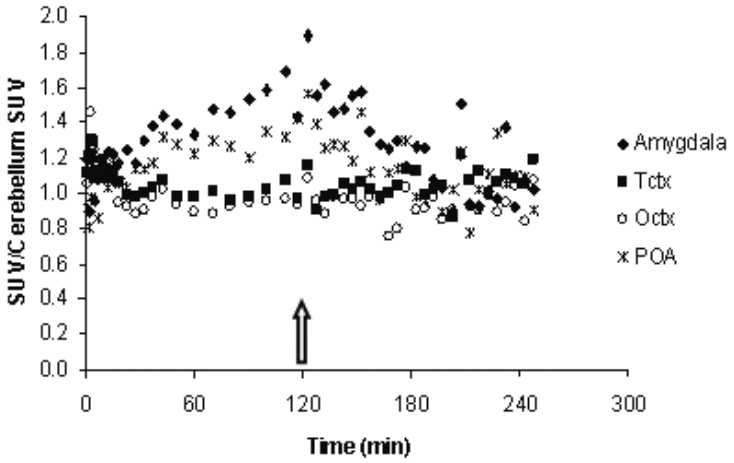

Figure 22. TAC of [^{18}F]FVOZ in the amygdala, TCTX, OCTX, and hypothalamus of a rhesus monkey, normalized by the SUV in the cerebellum. Unlabeled vorozole (100µg/kg) was administered after 120 min as indicated by the arrow.

Pilot human PET study with VOZ†

This is the preliminary part of a study to be followed by one with an increased number of patients and volunteers.

†Naessen T, Engler H, Takahashi K, Larsson M, Kirilovas D, Razifar P, Långström B. PET studies of brain aromatase in patients with long-term estrogen therapy. *Work in progress*, 2008.

To investigate the effect of long term estrogen treatment on aromatase expression in the brain, two female patients who had been treated with estrogen for more than five years and two age-matched female volunteers were examined with PET and VOZ. The subjects were given a bolus injection of 378±2.8 MBq VOZ, after which dynamic PET scans over the brain were acquired for 60 min. .

PET images indicating the distribution of VOZ binding are shown in Figure 23. In the human brain, high uptake of VOZ was observed in the thalamus. No strong signals were observed in the amygdala. The distribution pattern was similar between estrogen treated patients and age-matched volunteer. The number of subjects was too small to prove any statistical difference.

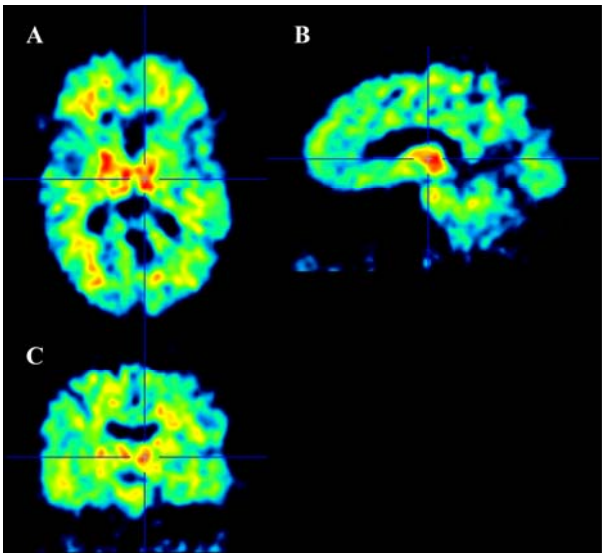

Figure 23. PET images of long-term estrogen-treated female brain. Cross hairs indicate the thalamus. A: Transaxial section including the thalamus region. B: Sagittal section indicated by the vertical line in panels A and C. C: Coronal section indicated by the horizontal line in panel A.

Discussion

Aromatase is one of the key enzymes involved in sex steroid balance, and its key role in the local generation of estrogens in the brain suggests that it might participate in the emotional status. This suggestion is reinforced by the observations that most types of anxiety disorders are more common among women than men [54-57] and ovariectomy increases anxiety and depression behavior [59-61]. Hence it is conceivable that changes in aromatase function or expression can play a role in mood disorders, either causative or as part of a compensatory and regulatory mechanism. Since there are only limited and only indirect alternative means to evaluate the role of aromatase in the living human brain, it is highly desirable to develop a PET tracer for qualification of aromatase, which could be used for noninvasive *in vivo* imaging. The PET technique, due to its versatility with respect to labeling of molecules and its very high sensitivity, is the logical choice to search for biological molecules that can be labeled for PET and used to demonstrate aromatase distribution in the living brain.

The tracer first used for aromatase imaging was VOZ. In our laboratory, the effects of androgens or follicular fluid from patients with polycystic ovary syndrome on aromatase activity had been investigated with VOZ [101]. This tracer has high affinity and specificity for aromatase, penetrates the blood-brain barrier (BBB), and reaches equilibrium with respect to binding within 20 min. The rate of metabolism *in vivo* is moderate, with the fraction of intact tracer in plasma being 85, 77, and 68% at 10, 20, and 45 min, respectively, after injection. These features are satisfactory for a good PET tracer. To be useful in neurobiology research, it is important that the tracer binding to its target can be quantified with reasonable effort, with reasonable precision, and generates values that are representative for the biological/physiological parameter explored. For the analysis of PET data in the first study (Paper I), a reference tissue model was selected due to the technical difficulty at that time to perform arterial blood sampling and metabolite analysis. Usually kinetic modeling needs the inclusion of a metabolite-corrected arterial input function; however, to obtain that requires an invasive and demanding procedure. The reference tissue model does not need blood sampling and instead uses the time activity curve of a reference tissue which is free from specific target proteins. Reference tissue methods are not able to provide a full kinetic analysis, but assuming certain relations between the kinetics of the tissue of interest and the reference tissue, they can provide

adequate measures of binding parameters. In the first study (Paper I), the cerebellum was used as a reference tissue for the evaluation, since aromatase mRNA and activity have been shown to be undetectable or negligibly small in the cerebellum of the adult rhesus monkey brain [7].

Our first attempt to image the monkey brain with PET and VOZ (Paper I) demonstrated a strong signal in the amygdala and a weaker one in the hypothalamus in only two of four monkeys. This result did not seem to agree with earlier reports that demonstrated aromatase mRNA and activity in the amygdala and hypothalamus in the male rhesus monkey [7]. In our second attempt to image the monkey brain with PET (Paper IV), VOZ binding was observed in the amygdala and hypothalamus before nandrolone treatment. This difference might be explained by sex differences in aromatase expression. The monkeys used in Paper I were females, whereas in paper IV we used males. Earlier reports [20,102] and our results from Paper I illustrated that female monkeys had a significantly lower level of aromatase in the CNS than male ones. These earlier studies were performed in rats; however, since the distribution and activity of aromatase show a similar pattern in rat and monkey, it is plausible to assume that female monkeys have a lower level of aromatase in the hypothalamus than males. Another possibility is that the differences seen in the two papers are attributable to technical factors, as different PET scanners were used. The PET scanners utilized in Paper I were GE PC 4096 (GEMS) and SHR-7700 (Hamamatsu Photonics KK) and their resolutions were 6 and 2.6 mm, respectively [103,104]. The resolution of the PET scanner used in Paper IV (microPET Focus 220, Siemens) was less than 2 mm [105].

The pattern of regional specific binding of VOZ shown in the *in vivo* studies using primates was confirmed by the *in vitro* studies using rats. *In vitro* autoradiography presented in Paper I demonstrated a high specific binding of VOZ in the BST and MA and a weak signal in the MPO. These regions are reported to contain high levels of aromatase mRNA [106,107] and show high aromatase activity in the rat brain [20]. High levels of aromatase activity were also found in the hypothalamus, and so it is not clear why our studies did not show a high specific binding of VOZ in the hypothalamus in the rat brain. VOZ binding may be less sensitive to aromatase than probes used in other techniques since the level of aromatase activity [40] or the amount of mRNA [106] is in the rank order of BST>MA>hypothalamic area. The autoradiography in Paper I also showed that VOZ binding differed significantly between the sexes. In all three regions in which specific binding was observed (*i.e.*, MA, BST, and MPO), females had significantly lower binding than males. This result agrees with some earlier reports [20,102], but other reports failed to show a sex difference in the MA [40,106,108,109]. However, the reports showing no sex difference in the MA demonstrated that females had a tendency to have lower levels of aromatase, although the difference between sexes did not reach statistical significance. Thus, the sex

difference in the MA is still an unsettled issue and could depend on the method used, individuals, and other factors in the experiments. The estrous cycle in females does not seem to influence aromatase activity in the brain [40].

In the Scatchard plot analysis of the homogenate binding study, a linear fit was obtained, indicating that aromatase has a single binding site for VOZ. This finding is consistent with a report showing that vorozole, other non-steroidal aromatase inhibitors (fadrozole, liazole and aminoglutethimide) and a natural substrate androstenedione bound to aromatase in a similar way and interacted with the I-helix and C-terminus of aromatase [19]. Our Scatchard plot analysis revealed a K_D of 0.60 nM for vorozole binding to aromatase in the MA of rats. This value is not far from aromatase inhibition constants for vorozole found previously in several *in vitro* systems [5,85,87,110-112].

These *in vivo* and *in vitro* studies revealed that the PET tracer VOZ had a high affinity and specificity for brain aromatase and could thus have a potential for *in vivo* aromatase imaging. Application to AAS abuse became the next step in our exploration of VOZ.

The biochemistry of AAS abuse is not fully understood. The potential that androgens can be converted to estrogens in focal regions of the brain, and that there could therefore be a potential role of aromatase in the neuronally-mediated effects of steroid abuse motivated us to explore the effects of AAS abuse on aromatase by utilizing our new tool, VOZ. In Papers II and III, the effect of chronic treatment with nandrolone on aromatase in the male rat brain was studied by using VOZ. A supraphysiological dose of nandrolone (15 mg/kg) was chosen to mimic heavy AAS abuse in humans. The doses of AAS used by steroid abusers are frequently over 10-100-fold greater than the clinical doses [113]. In the case of AAS abuse in humans, the weekly dosage of AAS is mostly in the range of 500-1500 mg [114]. A clinically relevant dose is 1.0-3.0 mg/kg/day when the body weight is around 80 kg. On the basis of this dosage and taking into consideration species differences, we used a dose of 15 mg/kg/day to simulate a rather heavy AAS abuse in rats in Paper II. In Paper III, however, the ethics committee indicated that the frequency of injection should be reduced to avoid a local inflammation at the injection site, and thus the dose in Paper III was chosen to be 15 mg/kg once every 3 days.

The results of Papers II and III were qualitatively congruent. An increase in VOZ binding to aromatase in the BST and MPO was observed after nandrolone treatment. On the other hand, no change was observed in the MA. The degree of increase in VOZ binding in the BST and MPO by nandrolone was 45 and 81%, respectively, in Paper II, but only 15 and 34% in Paper III. The lower degree of increase in binding found in Paper III may have been because of the use of a different procedure for treatment. In Paper II, the rats were given daily intramuscular injections of nandrolone (15 mg/kg) for 14 days, whereas in Paper III, the rats were treated subcutaneously (15 mg/kg)

once every 3 days for 20 days. The cumulative dose was thus twice as high in Paper II, 210 mg/kg, as in Paper III, 105 mg/kg. It is fully conceivable that the lower degree of increase in VOZ binding with nandrolone treatment in Paper III was due to the more moderate exposure than that in Paper II.

The increase in VOZ binding in the BST and MPO by nandrolone treatment in Paper II suggested that androgen is a regulator of the central aromatization at the protein expression level. Earlier reports support this notion; *i.e.*, the concentration of aromatase mRNA and aromatase activity decreased in the MPO following castration and testosterone treatment restored it to normal levels [115], and AR-deficient, testicular feminized rats had a lower aromatase activity in their MPO than normal littermates [116]. Nandrolone has a higher affinity for the AR than testosterone does [117], and thus the more potent androgen (nandrolone) could evoke an up-regulation of aromatase, which might be the reason for the higher specific binding of VOZ in nandrolone-treated rats observed in Paper II.

In order to investigate if the aromatase up-regulation by androgens was exerted via the AR, flutamide treatment was added to the nandrolone treatment in Paper III. Flutamide is an AR antagonist and inhibits the biologic effects of androgens. Flutamide treatment suppressed aromatase expression in the BST, MPO and MA. The degree of suppression by flutamide was similar in the control and the nandrolone groups, confirming that regulation of aromatase expression is at least partly mediated via ARs.

The MPO was the region most influenced by nandrolone and flutamide treatment, and this finding suggests that aromatase in the MPO is sensitive to androgens through ARs, a view taken by earlier reports [109,115-118].

Certain limbic structures, namely, the BST and amygdala, have been reported not to be sensitive to androgens. The limbic structures were unresponsive to gonadectomy [119], and androgens did not regulate aromatase activity in the medial and cortical amygdala [41]. However, testosterone target neurons were found to be abundant in the MPO and BST [120]; and thus the BST can also be considered to be regulated by androgens. In addition, there is a report showing that aromatase activity in the amygdala of testicular feminized rats was significantly lower than that in normal littermates and that aromatase activity in the BST of testicular feminized rats was lower than that in normal littermates [116]. These facts agree with our results in Papers II and III which illustrated that flutamide decreased specific binding of VOZ in the MA and BST, whereas nandrolone increased specific binding in the BST. These findings suggest that aromatase in the MA might also be regulated to a small extent by an AR-mediated mechanism, in line with the demonstration by several studies of a tendency in this direction, though it did not reach statistical significance [40,41]. Mathias et al. reported that flutamide treatment and castration affected aromatase activity in different fashions in different strains of rats [121]. Although the aromatase activity in the amygdala of Norway Brown and Wistar rats was unaffected

by castration, that in the amygdala of Sprague-Dawley rats tended to be reduced both by flutamide treatment and castration compared with the control value ($P<0.06$). In the studies in Paper III we employed Sprague-Dawley rats, and the decrease observed in the MA might have been specific to this rat strain.

In any case, it seems that there are different systems by which androgens regulate aromatase in these three regions. To clarify this, more research is required.

Although physiological concentrations of testosterone provoke neurite outgrowth [122], supraphysiological doses of it increase cytosolic calcium concentrations and induce apoptosis of neuronal cells [123]. Nandrolone, which is a derivative of testosterone with higher potency than testosterone, might therefore also have cytotoxic effects. In addition, since nandrolone can be aromatized to estradiol with up to 20% of the efficiency of testosterone [124], aromatase expression could be up-regulated to prevent cytotoxic effects. If heavy abuse of nandrolone has cytotoxic effects, it might be hypothesized that the increase in aromatase expression in neurons, which was demonstrated in Paper III, may counteract those effects, since estrogens, aromatized metabolites of androgens, are known to have neuroprotective effects [125]. Further research is needed to test this hypothesis of cytotoxicity.

Our evaluation of the effects of nandrolone on brain aromatase by using VOZ proceeded from *ex vivo* studies to true *in vivo* studies. Paper IV is the first report to observe AAS effects on brain aromatase using *in vivo* imaging with PET. The advantage of the PET technique is that it is non-invasive and yet allows a characterization of biochemistry and physiology; and, furthermore, the experimenter can repeat PET scans in the same individual, allowing the monitoring of changes with time or after different challenges within the same individual. To evaluate PET images, the LNIM was selected, since it does not require arterial blood sampling; and the DVR, which is calculated with this model, is frequently used as a parameter for comparison of studies using reversibly binding radiotracers [126-128] such as VOZ. LNIM needs a k'_2, an average tissue-to-plasma clearance, which can be calculated by SRTM or Ichise's multilinear reference tissue model [129] but can also be calculated by actual arterial blood sampling. In our study, arterial blood sampling succeeded once; and, therefore, we calculated k'_2 and confirmed the estimated k'_2 by SRTM.

The distribution of VOZ binding *in vivo* in our primates showed high levels of binding in the amygdala and hypothalamus. The BP in the amygdala did not change after nandrolone treatment, whereas the BP in the hypothalamus was increased by 71% after it ($P<0.05$). This result is in agreement with our studies using rats (Papers II and III). It is reported that brain aromatase activity and mRNA expression are regulated by testosterone and DHT in the rhesus monkey brain [21,130]. These reports also showed an

increased mRNA expression in the hypothalamus and no change in the amygdala. There might hence be different regulatory systems for aromatase in these two regions in monkeys as well as in rats.

The two monkeys that were scanned one month after the nandrolone treatment showed diverse results. It is difficult to speculate about this diversity, since the number of animals was only two. Further research with increased number of animals is obviously needed.

One of the objectives of our research was to generate new methods that can aid in the understanding of some of the emotional or behavioral effects of AAS, for example, aggression. In this respect it is interesting to note the pronounced up-regulation of aromatase in the BST and MPO. The hypothesis of a role for estrogens with respect to aggressive behavior is strengthened by observations of increased expression of ERα and decreased expression of ERβ in these same regions in mice exposed to short daylight periods, which increases aggression [131]. Another report noted that ERβ knockout mice exhibited enhanced anxiety and decreased concentrations of serotonin in several brain regions including the BST and MPO [132]. The biochemical interactions, however, observed thus far seem too complex to permit generation of a global theory of the mode of AAS in relation to aggression. A future task of great interest would be to explore whether pharmacological inhibition of aromatase would modulate AAS-induced aggression.

The AR is regulated by androgens, and AAS, which are more potent than testosterone, can increase the number of these receptors [133]. Other reports and our previous *in vitro* VOZ binding study suggested that aromatase expression was regulated through the AR [116]; *i.e.*, AAS induced an increase in ARs and consequently aromatase was up-regulated. Increased aromatase expression might induce over-production of estrogens, and these excess estrogens can reduce the number of ER [134].

Finally, to seek potential new PET probes for aromatase with better characteristics, two kinds of ^{18}F-labeled vorozole analogs were developed and characterized. Albeit VOZ has a good affinity and specificity, the characters of ^{18}F, especially the longer half life, are also favorable and useful. To use ^{11}C-labeled compounds, research centers or hospitals need to have their own cyclotrons; whereas ^{18}F-labeled compounds can be distributed to research centers or hospitals not equipped with cyclotrons. Moreover, a longer half life allows longer scan times, and this might enable an evaluation of late phenomena that cannot be captured with [^{11}C]-labeled compounds. Additionally these novel structures of ^{18}F-labeled vorozole analogues could potentially have other pharmacological properties that might suit certain other applications.

Both [^{18}F]FVOZ and [^{18}F]FVOO had good affinity and specificity, and particularly [^{18}F]FVOZ seemed to have superior properties. The K_D value of [^{18}F]FVOZ was 0.21 nM, which is in the range normally suited for PET studies, and this gives a 30-fold higher affinity than that of [^{18}F]FVOO and a

3-fold increased affinity compared with that of VOZ. In accordance with the VOZ studies, a specific binding of [^{18}F]FVOZ and [^{18}F]FVOO was found in the MA, BST and MPO *in vitro*. However, as [^{18}F]FVOO is metabolized quickly [98] and *ex vivo* autoradiography failed to show binding in the brain, [^{18}F]FVOO is not suitable for use *in vivo*.

The biodistribution studies showed, as previously observed with VOZ [5], a marked accumulation in the adrenal glands. Although not yet clarified, this might be related to binding to other enzymes in the steroid synthesis pathway. This binding to the adrenals was not blocked by pre-treatment with unlabeled vorozole, in contrast to that to the ovary, where an expected selective binding to aromatase should be at hand [5,135,136]. There was probably some defluorination in both [^{18}F]FVOZ and [^{18}F]FVOO, as the accumulation of radioactivity increased in bone with time.

The PET studies performed in the monkey with [^{18}F]FVOZ demonstrated a distribution pattern similar to that for VOZ, *i.e.*, specific binding in the amygdala and hypothalamus. The specific [^{18}F]FVOZ binding was rapidly and totally displaced by intravenous administration of unlabeled vorozole, thus indicating reversible binding and rapid kinetics.

Taken together, the data suggest that [^{18}F]FVOZ can a suitable tracer for further exploration by *in vitro* and *in vivo* studies aiming to define its role as an alternative to VOZ.

With the goal of imaging brain aromatase under different physiological conditions in humans, we have started a human PET study with long-term estrogen treatment. Although the number of subjects is too small, high VOZ-binding was observed in the thalamus. The distribution pattern of brain aromatase in humans might be different from that in rodents and monkeys. The aromatase in human brain has not been fully characterized yet, but with the PET technique, we may gain knowledge about the human enzyme that can not be obtained from animal models.

Summary

For the first time we have demonstrated the *in vivo* imaging of brain aromatase by using VOZ and PET. The distribution pattern of specific binding of VOZ was similar in an *in vitro* study using the rat brain and in an *in vivo* one usin the rhesus monkey brain, and specific binding was observed in the limbic and hypothalamic regions. The highest signal was found in the MA and the lowest in the MPO in both sexes of rat. In all three regions, males had higher signals than females. The K_D of VOZ binding to aromatase in the rat MA was determined to be 0.60 nM. These results are in agreement with earlier studies that determined aromatase distribution by different techniques and with the K_D value of unlabeled vorozole. Taken together, VOZ is a good PET tracer for *in vivo* aromatase imaging with a high affinity and sensitivity.

Next, this technique was applied to an investigation of brain aromatase under different physiological conditions, namely AAS abuse, with the goal of exploring one aspect of AAS abuse. Such abuse has become a social problem in Sweden as well as in the USA. In our experiments, an abuse level of AAS increased significantly the levels of aromatase in the BST and MPO, whereas in the MA it caused no significant change. These results indicate that the manner of regulation of aromatase protein expression might be different in the BST and MPO than in the MA. The alteration of the density of aromatase in the BST and MPO could explain some psychological features of AAS abusers.

In order to further explore the regulation of aromatase levels, we employed flutamide, an AR antagonist. This second AAS experiment also demonstrated that AAS up-regulated aromatase expression in the BST and MPO. In the same regions, flutamide treatment down-regulated aromatase expression. These results suggest that aromatase is regulated through an AR-mediated mechanism. The increase in aromatase expression was confined to neurons.

The investigation of aromatase levels affected by AAS was then turned to a higher species, the rhesus monkey. In this monkey, similar results as in rats were obtained. AAS treatment increased aromatase levels in the hypothalamus but not in the amygdale of these monkeys. This experiment was performed *in vivo* with PET, and thus these results reinforced the concept of AAS promotion of brain aromatase, which might be related to AAS abuser's mood instability.

Even though VOZ is a good PET tracer, we sought to develop an even better or a different one for aromatase. ^{18}F-labeled vorozole analogs may for certain applications have advantages due to the relative longer half-life of the radionuclide. This allows the tracer to be distributed to facilities without a cyclotron, and it means that the *in vivo* research on aromatase can performed on a wider scale. The two newly synthesized ^{18}F-labeled vorozole analogs, [^{18}F]FVOZ and [^{18}F]FVOO, displayed different characteristics. The distribution pattern of specific binding *in vitro* of each analog was similar to that of VOZ. A specific binding was visualized in the BST, MPO, and MA. However, *in vivo* [^{18}F]FVOO was metabolized very quickly, meaning that this tracer is not suitable as a PET ligand. Considering these results, [^{18}F]FVOZ can be an appropriate PET tracer and be an alternative or complement to VOZ.

We have just started PET studies using VOZ in human subjects. Such studies might help us to understand the function of aromatase in the complicated human brain. Aromatase, the enzyme converting androgens to estrogens, may play a role in mood and mood disorders. Emotions are the "spices" of life for us human beings but also a potential "curse." We hope that our studies may be a small further step towards the possibility of investigating and understanding this specific aspect of human beings.

Populärvetenskaplig sammanfattning på svenska

Aromatas är ett enzym som konverterar manliga könshormoner till kvinnliga hormoner och kan ha betydelse för humör och välbefinnade. Huvudtemat för avhandlingen är molekyl avbildning av enzymet aromatas i hjärnan med positron emissions tomografi (PET) teknik. PET är en icke-invasiv avbildnings-teknik som kan visualisera bindning till proteiner i levande individer. Spårmolekyler som märkts med radioaktivitet emitterar γ-strålning i målregioner. PET kameran registrerar γ-strålarna och gör bilder. Man kan se hur spår molekyler ackumulerar i målregioner. En spår molekyl för aromatas, [^{11}C]vorozole (VOZ), utvecklades och undersöktes med in vitro och in vivo metoder. In vitro experiment i rått-hjärna visade att VOZ bindning fanns i mediala amygdala, bed nucleus stria terminalis och mediala preoptic area som är kända aromatas rika regioner. K_D värdet för VOZ var 0.60 nM med en specific bindning till aromatas. PET studie i rhesus apa uppvisade högt upptag av VOZ i hypothalamus och amygdala. Dessa experiment indikerade att VOZ är en användbar PET substans för avbildning av aromatas.

Tekniken applicerades sedan till undersökning av aromatas i hjärnan under missbruk av anabola steroid. Missbruk av anabola steroider har blivit ett socialt problem i Sverige och världen Våra experiment visade att anabola steroider ökade VOZ bindningen i bed nucleus stria terminalis och mediala preoptic area, men gav ingen ändring i mediala amygdala. Det verkar vara olika reglerings-system i bed nucleus stria terminalis och mediala preoptic area, jämfört med mediala amygdala. [^{11}C]Vorozole bindningen minskade med flutamide behandling som blockerar receptorer för manliga hormoner , dvs ändringen i aromatas av anabola steroider sker genom androgen receptorer. PET studie med levande rhesus apa demonstrerade ökad VOZ bindning i hypothalamus av behandling med anabola steroider. Denna ändring av aromatas i hjärnan kan vara en av orsakerna till den psykologiska obalans som missbruk av anabola steroider leder till.

För att söka bättre eller andra typer av spårmolekyler för aromatas, utvecklade vi ^{18}F-märkta vorozole analoger. ^{18}F har längre halveringstid än ^{11}C, som gör det möjligt att skicka till annat facilitet som inte har cyklotron. Två olika ^{18}F-märkta vorozole analoger, [^{18}F]FVOZ och [^{18}F]FVOO

utvecklades, men [^{18}F]FVOO metaboliseras väldigt snabbt och passar inte som PET spårmolekyl. [^{18}F]FVOZ kan vara ett alternativ till VOZ.
Vilken roll aromatas spelar i human hjärna är fortfarande inte helt klar. PET tekniken med radioaktivt vorozole kan hjälpa att undersöka aromatas i human hjärna. Vi har precis börjat PET studies i människa vilket kan bli ett första steg att öka vår förståelse i det mest komplicerade organet: den mänskliga hjärnan.

Acknowledgements

It was not easy to make this thesis and took so long time for me to accomplish the works. Without the support from people who related to me in various ways, I could not have succeeded to make this thesis. I would like to express my appreciation to everyone, especially to the following people:

My supervisor, professor *Mats Bergström*, for encouraging and motivating me to challenge such an interesting work, and for understanding my traveling habitude. I felt your solicitude even after you (and I) left Sweden. I am grateful especially for your support at the last months to make this thesis.

Professor *Bengt Långström*, my other supervisor, for support my seven years in Sweden as my Swedish father. I was helped a lot by your enthusiastic but calm attitude when I faced with difficulties.

Professor *Yasuyoshi Watanabe*, my other supervisor, for giving me a chance to study and live in Sweden. I learned a lot of essences of life from you and met many wonderful people via you. I'm really enjoying to research at your institute now.

My co-authors, *Eva-Lotta Nyberg* for producing VOZ so many times, *Maria Erlandsson* for collaboration with FVOZ and FVOO, *Håkan Hall* and *Sergio Estrada* for complementing experiments after my leaving, and for nice discussion, and for being always very nice companies, *Pernilla Johansen* for metabolite analysis, *Mathias Hallberg*, *Kristina Magnusson* and *Fred Nyberg* for fruitful collaboration.

Elisabeth Bergström-Pettermann, for teaching me lab techniques, and for your warm heart and so helpful and cheerful characters. I always felt a great relief if you are just there.
System administrators, *Harald Schnider* for teaching me the operation of computer analyzing system, and for resolving problems with computers, *Lars Lindsjö* for handling data, *Tomas Nyberg* for supporting systems.

Nurses helped me at PET studies, especially *Mimmi Lidholm* and *Rita Öhrstedt* for helping clinical studies, *Gudrun Nylén* and *Urban Höglund* for helping monkey studies and being a good company, monkey specialists in Törneby for helping monkey studies.

Gábor Lendvai, for your tremendous kindness and for answering my too many questions, *Azita Monazzam*, for your warm heart, it was so nice to share the room with you, *Stina Syvänen*, for your brilliant mind and excellent advices, *Pasha Razifar*, for your skillfulness in various ways, *Irina Velikyan*, for your smart jokes and for being "broccoli and spaghetti" partner, *Henry Engler*, for your very warm personality, I always felt happy when I saw you, *Li Lu*, for your nice care for me and for very good "*jiaozi*", *Mark Lubberink*, for your nice personality and for the tour in Kyoto, *Julien Barletta*, for being a good company and for your knowledge about "*manga*", *Richard Torstenson*, for supervising my master work and for being like a big brother, you were the first impression as a Swedish man for me (and I learned that Swedish men love drinking and dancing), *Linda Samuelsson*, for your lovely personality and for kindness.

All past and present members at PET center/Uppsala Imanet and the pre-clinical lab., especially *Anders*, *Anders S*, *Anders W*, *Daniel J*, *Daniel L*, *Dimitrius*, *Eva*, *Farhad*, *Feng*, *Gunnar B*, *Helena*, *Ingalill*, *Irina S*, *Jens*, *Johanna*, *Jonas*, *Lieuwe*, *Madde*, *Maggan*, *Martin*, *Oleksiy*, *Padideh*, *Poppi*, *Robert*, *Sasha*, *Shaheena*, *Wiebke & Sven* , *Yvonne* and *Örjan* for nice companies and works.

Ulla Jonson, for kind helps on administration.

All Japanese friends I met in Sweden, especially *Nobuko & Koichi* for introduction of the life in Sweden and for excellent Japanese food, *Haruyo*, *Minako & Akio*, *Michiko*, *Miyuki*, *Hisashi*, *Kengo* for sharing happy time.

All members at Molecular Imaging Research Program, RIKEN, especially *Hirotaka Onoe*, for many advises and discussion on monkey studies, *Kayo Onoe*, for analyses of huge data, *Hiroko Nagata*, for production of tracers, *Tadayuki Takashima* for metabolite analyses, *Yasuhisa Tamura* for being a good company and for answering my stupid questions.

Masamune Kusano, for your melody and irresistible voice. Your voice saved me in dark and cold morning.

Hitoshi Matsumoto, for your gift of nature in comedy. Thanks to your DVDs, I could survive in the world only with Western comedy.

Yasuko, *Yuchiko*, *Masumi*, for being the best friends for 20 years, *Setsu & Akira*, for very nice care for me.

Yah, for your tremendous and endless support and care for me.

My parents, *Toshiko & Akira*, and “down-to-earth” brother, *Kazuo*, for support and understanding.

References

1. Lephart ED. A review of brain aromatase cytochrome P450. *Brain Research Reviews* 1996; 22:1-26.
2. Naftolin F, Ryan KJ, Petro Z. Aromatization of androstenedione by limbic system tissue from human foetuses. *J. Endocrinol.* 1971; 51:795-796.
3. Naftolin F, Ryan KJ, Petro Z. Aromatization of androstenedione by the diencephalon. *J. Clin. Endocrinol. Metab.* 1971; 33:368-370.
4. Fink G, Sumner BE, McQueen JK, Wilson H, Rosie R. Sex steroid control of mood, mental state and memory. *Clin. Exp. Pharmacol. Physiol.* 1998; 25:764-775.
5. Lidström P, Bonasera TA, Kirilovas D, et al. Synthesis, in vivo rhesus monkey biodistribution and in vitro evaluation of a ^{11}C-labelled potent aromatase inhibitor: [N-methyl-^{11}C]vorozole. *Nucl. Med. Biol.* 1998; 25:497-501.
6. Corbin CJ, Graham-Lorence S, McPhaul M, Mason JI, Mendelson CR, Simpson ER. Isolation of a full-length cDNA insert encoding human aromatase system cytochrome P-450 and its expression in nonsteroidogenic cells. *Proc. Natl. Acad. Sci. U. S. A.* 1988; 85:8948-8952.
7. Abdelgadir SE, Roselli CE, Choate JV, Resko JA. Distribution of aromatase cytochrome P450 messenger ribonucleic acid in adult rhesus monkey brains. *Biol. Reprod.* 1997; 57:772-777.
8. Hickey GJ, Krasnow JS, Beattie WG, Richards JS. Aromatase cytochrome P450 in rat ovarian granulosa cells before and after luteinization: adenosine 3',5'-monophosphate-dependent and independent regulation. Cloning and sequencing of rat aromatase cDNA and 5' genomic DNA. *Mol. Endocrinol.* 1990; 4:3-12.
9. Lephart ED, Peterson KG, Noble JF, George FW, McPhaul MJ. The structure of cDNA clones encoding the aromatase P-450 isolated from a rat Leydig cell tumor line demonstrates differential processing of aromatase mRNA in rat ovary and a neoplastic cell line. *Mol. Cell. Endocrinol.* 1990; 70:31-40.
10. Terashima M, Toda K, Kawamoto T, et al. Isolation of a full-length cDNA encoding mouse aromatase P450. *Arch. Biochem. Biophys.* 1991; 285:231-237.
11. McPhaul MJ, Noble JF, Simpson ER, Mendelson CR, Wilson JD. The expression of a functional cDNA encoding the chicken cytochrome P-450arom (aromatase) that catalyzes the formation of estrogen from androgen. *J. Biol. Chem.* 1988; 263:16358-16363.

12. Harada N, Yamada K, Foidart A, Balthazart J. Regulation of aromatase cytochrome P-450 (estrogen synthetase) transcripts in the quail brain by testosterone. *Brain Res. Mol. Brain Res.* 1992; 15:19-26.
13. Shen P, Campagnoni CW, Kampf K, Schlinger BA, Arnold AP, Campagnoni AT. Isolation and characterization of a zebra finch aromatase cDNA: in situ hybridization reveals high aromatase expression in brain. *Brain Res. Mol. Brain Res.* 1994; 24:227-237.
14. Hinshelwood MM, Corbin CJ, Tsang PC, Simpson ER. Isolation and characterization of a complementary deoxyribonucleic acid insert encoding bovine aromatase cytochrome P450. *Endocrinology* 1993; 133:1971-1977.
15. Tanaka M, Telecky TM, Fukada S, Adachi S, Chen S, Nagahama Y. Cloning and sequence analysis of the cDNA encoding P-450 aromatase (P450arom) from a rainbow trout (Oncorhynchus mykiss) ovary; relationship between the amount of P450arom mRNA and the production of oestradiol-17 beta in the ovary. *J. Mol. Endocrinol.* 1992; 8:53-61.
16. Trant JM. Isolation and characterization of the cDNA encoding the channel catfish (Ictalurus punctatus) form of cytochrome P450arom. *Gen. Comp. Endocrinol.* 1994; 95:155-168.
17. Simpson ER, Mahendroo MS, Means GD, Kilgore MW, Corbin CJ, Mendelson CR. Tissue-specific promoters regulate aromatase cytochrome P450 expression. *J. Steroid Biochem. Mol. Biol.* 1993; 44:321-330.
18. Simpson ER, Mahendroo MS, Means GD, et al. Aromatase cytochrome P450, the enzyme responsible for estrogen biosynthesis. *Endocr. Rev.* 1994; 15:342-355.
19. Koymans LM, Moereels H, Vanden Bossche H. A molecular model for the interaction between vorozole and other non-steroidal inhibitors and human cytochrome P450 19 (P450 aromatase). *J. Steroid Biochem. Mol. Biol.* 1995; 53:191-197.
20. Roselli CE, Horton LE, Resko JA. Distribution and regulation of aromatase activity in the rat hypothalamus and limbic system. *Endocrinology* 1985; 117:2471-2477.
21. Roselli CE, Stadelman H, Horton LE, Resko JA. Regulation of androgen metabolism and luteinizing hormone-releasing hormone content in discrete hypothalamic and limbic areas of male rhesus macaques. *Endocrinology* 1987; 120:97-106.
22. Roselli CE, Stormshak F, Resko JA. Distribution and regulation of aromatase activity in the ram hypothalamus and amygdala. *Brain Res.* 1998; 811:105-110.
23. Selmanoff MK, Brodkin LD, Weiner RI, Siiteri PK. Aromatization and 5alpha-reduction of androgens in discrete hypothalamic and limbic regions of the male and female rat. *Endocrinology* 1977; 101:841-848.

24. Evrard HC. Estrogen synthesis in the spinal dorsal horn: a new central mechanism for the hormonal regulation of pain. *Am. J. Physiol. Regul. Integr. Comp. Physiol.* 2006; 291:R291-299.
25. Hojo Y, Hattori TA, Enami T, et al. Adult male rat hippocampus synthesizes estradiol from pregnenolone by cytochromes P45017alpha and P450 aromatase localized in neurons. *Proc. Natl. Acad. Sci. U. S. A.* 2004; 101:865-870.
26. Horvath TL, Wikler KC. Aromatase in developing sensory systems of the rat brain. *J. Neuroendocrinol.* 1999; 11:77-84.
27. MacLusky NJ, Walters MJ, Clark AS, Toran-Allerand CD. Aromatase in the cerebral cortex, hippocampus, and mid-brain: ontogeny and developmental implications. *Mol. Cell. Neurosci.* 1994; 5:691-698.
28. Yague JG, Munoz A, de Monasterio-Schrader P, Defelipe J, Garcia-Segura LM, Azcoitia I. Aromatase expression in the human temporal cortex. *Neuroscience* 2006; 138:389-401.
29. Garcia-Segura LM, Wozniak A, Azcoitia I, Rodriguez JR, Hutchison RE, Hutchison JB. Aromatase expression by astrocytes after brain injury: implications for local estrogen formation in brain repair. *Neuroscience* 1999; 89:567-578.
30. Stein DG. Brain damage, sex hormones and recovery: a new role for progesterone and estrogen? *Trends Neurosci.* 2001; 24:386-391.
31. Garcia-Segura LM, Azcoitia I, DonCarlos LL. Neuroprotection by estradiol. *Prog. Neurobiol.* 2001; 63:29-60.
32. Azcoitia I, Doncarlos LL, Garcia-Segura LM. Estrogen and brain vulnerability. *Neurotoxicity Research* 2002; 4:235-245.
33. George FW, Ojeda SR. Changes in aromatase activity in the rat brain during embryonic, neonatal, and infantile development. *Endocrinology* 1982; 111:522-529.
34. Lephart ED, Simpson ER, McPhaul MJ, Kilgore MW, Wilson JD, Ojeda SR. Brain aromatase cytochrome P-450 messenger RNA levels and enzyme activity during prenatal and perinatal development in the rat. *Brain Res. Mol. Brain Res.* 1992; 16:187-192.
35. MacLusky NJ, Philip A, Hurlburt C, Naftolin F. Estrogen formation in the developing rat brain: sex differences in aromatase activity during early post-natal life. *Psychoneuroendocrinology* 1985; 10:355-361.
36. Tobet SA, Baum MJ, Tang HB, Shim JH, Canick JA. Aromatase activity in the perinatal rat forebrain: effects of age, sex and intrauterine position. *Brain Res.* 1985; 355:171-178.
37. Beyer C, Wozniak A, Hutchison JB. Sex-specific aromatization of testosterone in mouse hypothalamic neurons. *Neuroendocrinology* 1993; 58:673-681.
38. Compaan JC, Wozniak A, De Ruiter AJ, Koolhaas JM, Hutchison JB. Aromatase activity in the preoptic area differs between aggressive and nonaggressive male house mice. *Brain Res. Bull.* 1994; 35:1-7.

39. Wozniak A, Hutchison RE, Hutchison JB. Localisation of aromatase activity in androgen target areas of the mouse brain. *Neurosci. Lett.* 1992; 146:191-194.
40. Roselli CE, Ellinwood WE, Resko JA. Regulation of brain aromatase activity in rats. *Endocrinology* 1984; 114:192-200.
41. Roselli CE, Resko JA. Aromatase activity in the rat brain: hormonal regulation and sex differences. *J. Steroid Biochem. Mol. Biol.* 1993; 44:499-508.
42. Naftolin F, Ryan KJ, Petro Z. Aromatization of androstenedione by the anterior hypothalamus of adult male and female rats. *Endocrinology* 1972; 90:295-298.
43. Jones ME, Boon WC, Proietto J, Simpson ER. Of mice and men: the evolving phenotype of aromatase deficiency. *Trends in Endocrinology and Metabolism* 2006; 17:55-64.
44. Toda K, Saibara T, Okada T, Onishi S, Shizuta Y. A loss of aggressive behaviour and its reinstatement by oestrogen in mice lacking the aromatase gene (Cyp19). *J. Endocrinol.* 2001; 168:217-220.
45. Rochira V, Balestrieri A, Madeo B, Spaggiari A, Carani C. Congenital estrogen deficiency in men: a new syndrome with different phenotypes; clinical and therapeutic implications in men. *Mol. Cell. Endocrinol.* 2002; 193:19-28.
46. Carani C, Qin K, Simoni M, et al. Effect of testosterone and estradiol in a man with aromatase deficiency. *N. Engl. J. Med.* 1997; 337:91-95.
47. Herrmann BL, Saller B, Janssen OE, et al. Impact of estrogen replacement therapy in a male with congenital aromatase deficiency caused by a novel mutation in the CYP19 gene. *J. Clin. Endocrinol. Metab.* 2002; 87:5476-5484.
48. Maffei L, Murata Y, Rochira V, et al. Dysmetabolic syndrome in a man with a novel mutation of the aromatase gene: effects of testosterone, alendronate, and estradiol treatment. *J. Clin. Endocrinol. Metab.* 2004; 89:61-70.
49. Morishima A, Grumbach MM, Simpson ER, Fisher C, Qin K. Aromatase deficiency in male and female siblings caused by a novel mutation and the physiological role of estrogens. *J. Clin. Endocrinol. Metab.* 1995; 80:3689-3698.
50. Rochira V, Granata AR, Madeo B, Zirilli L, Rossi G, Carani C. Estrogens in males: what have we learned in the last 10 years? *Asian Journal of Andrology* 2005; 7:3-20.
51. Earls F. Sex differences in psychiatric disorders: origins and developmental influences. *Psychiatr. Dev.* 1987; 5:1-23.
52. Kessler RC, McGonagle KA, Swartz M, Blazer DG, Nelson CB. Sex and depression in the National Comorbidity Survey. I: Lifetime prevalence, chronicity and recurrence. *J. Affect. Disord.* 1993; 29:85-96.
53. Nolen-Hoeksema S. Sex differences in unipolar depression: evidence and theory. *Psychol. Bull.* 1987; 101:259-282.

54. Breslau N, Schultz L, Peterson E. Sex differences in depression: a role for preexisting anxiety. *Psychiatry Res.* 1995; 58:1-12.
55. Kessler RC, McGonagle KA, Zhao S, et al. Lifetime and 12-month prevalence of DSM-III-R psychiatric disorders in the United States. Results from the National Comorbidity Survey. *Arch. Gen. Psychiatry* 1994; 51:8-19.
56. Schneier FR, Johnson J, Hornig CD, Liebowitz MR, Weissman MM. Social phobia. Comorbidity and morbidity in an epidemiologic sample. *Arch. Gen. Psychiatry* 1992; 49:282-288.
57. Seeman MV. Psychopathology in women and men: focus on female hormones. *Am. J. Psychiatry* 1997; 154:1641-1647.
58. Smith RN, Studd JW, Zamblera D, Holland EF. A randomised comparison over 8 months of 100 micrograms and 200 micrograms twice weekly doses of transdermal oestradiol in the treatment of severe premenstrual syndrome. *Br J Obstet Gynaecol* 1995; 102:475-484.
59. Bowman RE, Ferguson D, Luine VN. Effects of chronic restraint stress and estradiol on open field activity, spatial memory, and monoaminergic neurotransmitters in ovariectomized rats. *Neuroscience* 2002; 113:401-410.
60. Estrada-Camarena E, Fernandez-Guasti A, Lopez-Rubalcava C. Antidepressant-like effect of different estrogenic compounds in the forced swimming test. *Neuropsychopharmacology* 2003; 28:830-838.
61. Walf AA, Rhodes ME, Frye CA. Antidepressant effects of ERbeta-selective estrogen receptor modulators in the forced swim test. *Pharmacol. Biochem. Behav.* 2004; 78:523-529.
62. Galea LA, Wide JK, Barr AM. Estradiol alleviates depressive-like symptoms in a novel animal model of post-partum depression. *Behav. Brain Res.* 2001; 122:1-9.
63. Farde L, Hall H, Ehrin E, Sedvall G. Quantitative analysis of D2 dopamine receptor binding in the living human brain by PET. *Science* 1986; 231:258-261.
64. Mathis CA, Wang Y, Holt DP, Huang GF, Debnath ML, Klunk WE. Synthesis and evaluation of ^{11}C-labeled 6-substituted 2-arylbenzothiazoles as amyloid imaging agents. *J. Med. Chem.* 2003; 46:2740-2754.
65. Fowler JS, MacGregor RR, Wolf AP, et al. Mapping human brain monoamine oxidase A and B with ^{11}C-labeled suicide inactivators and PET. *Science* 1987; 235:481-485.
66. Bergstrom M, Westerberg G, Nemeth G, et al. MAO-A inhibition in brain after dosing with esuprone, moclobemide and placebo in healthy volunteers: in vivo studies with positron emission tomography. *Eur. J. Clin. Pharmacol.* 1997; 52:121-128.
67. Orlefors H, Sundin A, Fasth KJ, et al. Demonstration of high monoaminoxidase-A levels in neuroendocrine gastroenteropancreatic tumors in vitro and in vivo-tumor visualization using positron emis-

sion tomography with ^{11}C-harmine. *Nucl. Med. Biol.* 2003; 30:669-679.
68. Bergstrom M, Bonasera TA, Lu L, et al. In vitro and in vivo primate evaluation of carbon-11-etomidate and carbon-11-metomidate as potential tracers for PET imaging of the adrenal cortex and its tumors. *J. Nucl. Med.* 1998; 39:982-989.
69. Varga I, Racz K, Kiss R, et al. Direct inhibitory effect of etomidate on corticosteroid secretion in human pathologic adrenocortical cells. *Steroids* 1993; 58:64-68.
70. Weber MM, Lang J, Abedinpour F, Zeilberger K, Adelmann B, Engelhardt D. Different inhibitory effect of etomidate and ketoconazole on the human adrenal steroid biosynthesis. *Clin. Investig.* 1993; 71:933-938.
71. Bergstrom M, Juhlin C, Bonasera TA, et al. PET imaging of adrenal cortical tumors with the 11beta-hydroxylase tracer ^{11}C-metomidate. *J. Nucl. Med.* 2000; 41:275-282.
72. Bauer M, Wagner CC, Langer O. Microdosing studies in humans: the role of positron emission tomography. *Drugs R D* 2008; 9:73-81.
73. Bjurling P, Watanabe Y, Malmborg P, Langstrom B. Multienzymatic syntheses of some ^{11}C-labelled neurotransmitter precursors: tyrosine, DOPA, tryptophan and 5-hydroxytryptophan. *J. Label. Compd. Radiopharm.* 1989; 26:243-246.
74. Orlefors H, Sundin A, Ahlstrom H, et al. Positron emission tomography with 5-hydroxytryprophan in neuroendocrine tumors. *J. Clin. Oncol.* 1998; 16:2534-2541.
75. Eriksson O, Wall A, Marteinsdottir I, et al. Mood changes correlate to changes in brain serotonin precursor trapping in women with premenstrual dysphoria. *Psychiatry Res* 2006; 146:107-116.
76. Torstenson R, Hartvig P, Langstrom B, Westerberg G, Tedroff J. Differential effects of levodopa on dopaminergic function in early and advanced Parkinson's disease. *Ann. Neurol.* 1997; 41:334-340.
77. Dence CS, Napolitano E, Katzenellenbogen JA, Welch MJ. Carbon-11-labeled estrogens as potential imaging agents for breast tumors. *Nucl. Med. Biol.* 1996; 23:491-496.
78. van Haver D, Vandecasteele C, Vandewalle T, Vandecasteele C. Production of ^{11}C-labeled quinidine and tamoxifen. *J. Label. Compd. Radiopharm.* 1985; 22:535-545.
79. Hostetler ED, Jonson SD, Welch MJ, Katzenellenbogen JA. Synthesis of 2-[(18)F]fluoroestradiol, a potential diagnostic imaging agent for breast cancer: Strategies to achieve nucleophilic substitution of an electron-rich aromatic ring with [(18)F]F(-). *J. Org. Chem.* 1999; 64:178-185.
80. Romer J, Fuchtner F, Steinbach J. Synthesis of 16alpha-[^{18}F]fluoroestradiol-3, 17beta-disulphamate. *J. Label. Compd. Radiopharm.* 2000; 43:425-436.
81. Garg PK, Labaree DC, Hoyte RM, Hochberg RB. [7alpha-^{18}F]fluoro-17alpha-methyl-5alpha-dihydrotestosterone: a ligand for

androgen receptor-mediated imaging of prostate cancer. *Nucl. Med. Biol.* 2001; 28:85-90.
82. Liu AJ, Katzenellenbogen JA, VanBrocklin HF, Mathias CJ, Welch MJ. 20-[^{18}F]fluoromibolerone, a positron-emitting radiotracer for androgen receptors: synthesis and tissue distribution studies. *J Nucl Med* 1991; 32:81-88.
83. Tagnon HJ. Antiestrogens in treatment of breast cancer. *Cancer* 1977; 39:2959-2964.
84. De Coster R, Wouters W, Bowden CR, et al. New non-steroidal aromatase inhibitors: focus on R76713. *J. Steroid Biochem. Mol. Biol.* 1990; 37:335-341.
85. Vanden Bossche H, Willemsens G, Roels I, et al. R 76713 and enantiomers: selective, nonsteroidal inhibitors of the cytochrome P450-dependent oestrogen synthesis. *Biochem. Pharmacol.* 1990; 40:1707-1718.
86. Wouters W, Snoeck E, De Coster R. Vorozole, a specific non-steroidal aromatase inhibitor. *Breast Cancer Res. Treat.* 1994; 30:89-94.
87. Wouters W, Van Ginckel R, Krekels M, Bowden C, De Coster R. Pharmacology of vorozole. *J. Steroid Biochem. Mol. Biol.* 1993; 44:617-621.
88. Plourde PV, Dyroff M, Dukes M. Arimidex: a potent and selective fourth-generation aromatase inhibitor. *Breast Cancer Res. Treat.* 1994; 30:103-111.
89. Bhatnagar AS, Hausler A, Schieweck K, Lang M, Bowman R. Highly selective inhibition of estrogen biosynthesis by CGS 20267, a new non-steroidal aromatase inhibitor. *J. Steroid Biochem. Mol. Biol.* 1990; 37:1021-1027.
90. Iveson TJ, Smith IE, Ahern J, Smithers DA, Trunet PF, Dowsett M. Phase I study of the oral nonsteroidal aromatase inhibitor CGS 20267 in postmenopausal patients with advanced breast cancer. *Cancer Res.* 1993; 53:266-270.
91. Goss PE, Winer EP, Tannock IF, Schwartz LH. Randomized phase III trial comparing the new potent and selective third-generation aromatase inhibitor vorozole with megestrol acetate in postmenopausal advanced breast cancer patients. North American Vorozole Study Group. *J. Clin. Oncol.* 1999; 17:52-63.
92. Kindlundh AM, Isacson DG, Berglund L, Nyberg F. Factors associated with adolescent use of doping agents: anabolic-androgenic steroids. *Addiction* 1999; 94:543-553.
93. Bahrke MS, Yesalis CE, Brower KJ. Anabolic-androgenic steroid abuse and performance-enhancing drugs among adolescents. *Child Adolesc. Psychiatr. Clin. N. Am.* 1998; 7:821-838.
94. Lindqvist AS, Johansson-Steensland P, Nyberg F, Fahlke C. Anabolic androgenic steroid affects competitive behaviour, behavioural response to ethanol and brain serotonin levels. *Behav. Brain Res.* 2002; 133:21-29.

95. Johansson-Steensland P, Nyberg F, Chahl L. The anabolic androgenic steroid, nandrolone decanoate, increases the density of Fos-like immunoreactive neurons in limbic regions of guinea-pig brain. *Eur. J. Neurosci.* 2002; 15:539-544.
96. Le Greves P, Huang W, Johansson P, Thornwall M, Zhou Q, Nyberg F. Effects of an anabolic-androgenic steroid on the regulation of the NMDA receptor NR1, NR2A and NR2B subunit mRNAs in brain regions of the male rat. *Neurosci. Lett.* 1997; 226:61-64.
97. Hallberg M, Johansson P, Kindlundh AM, Nyberg F. Anabolic-androgenic steroids affect the content of substance P and substance P(1-7) in the rat brain. *Peptides* 2000; 21:845-852.
98. Erlandsson M, Karimi F, Takahashi K, Langstrom B. ^{18}F-Labelled vorozole analogues as PET tracer for aromatase. *J. Label. Compd. Radiopharm.* 2008; 51:207-212.
99. Lammertsma AA, Hume SP. Simplified reference tissue model for PET receptor studies. *Neuroimage* 1996; 4:153-158.
100. Logan J, Fowler JS, Volkow ND, Wang GJ, Ding YS, Alexoff DL. Distribution volume ratios without blood sampling from graphical analysis of PET data. *J. Cereb. Blood Flow Metab.* 1996; 16:834-840.
101. Kirilovas D. Regulation of ovarian aromatase: Studies by aromatase assays in vitro and in vivo. In Faculty of Medicine. Uppsala: Uppsala University; 2003.
102. Roselli CE, Resko JA. The distribution and regulation of aromatase activity in the central nervous system. *Steroids* 1987; 50:495-508.
103. Rota Kops E, Herzog H, Schmid A, Holte S, Feinendegen LE. Performance characteristics of an eight-ring whole body PET scanner. *J. Comput. Assist. Tomogr.* 1990; 14:437-445.
104. Watanabe M, Okada H, Shimizu K, et al. A high resolution animal PET scanner using compact PS-PMT detectors. *IEEE Transactions on Nuclear Science* 1997; 44.
105. Jan S, Comtat C, Boisgard R, Trebossen R. Comparative study of microPET/spl reg/Focus and ECAT HRRT PET systems for small rodents imaging. *Nuclear Science Symposium Conference Record* 2004; 6:3430-3432.
106. Roselli CE, Abdelgadir SE, Ronnekleiv OK, Klosterman SA. Anatomic distribution and regulation of aromatase gene expression in the rat brain. *Biol. Reprod.* 1998; 58:79-87.
107. Wagner CK, Morrell JI. Neuroanatomical distribution of aromatase MRNA in the rat brain: indications of regional regulation. *J. Steroid Biochem. Mol. Biol.* 1997; 61:307-314.
108. Roselli CE. Sex differences in androgen receptors and aromatase activity in microdissected regions of the rat brain. *Endocrinology* 1991; 128:1310-1316.
109. Roselli CE, Abdelgadir SE, Resko JA. Regulation of aromatase gene expression in the adult rat brain. *Brain Res. Bull.* 1997; 44:351-357.

110. Krekels MD, Wouters W, De Coster R. Aromatase inhibition by R 76 713: a kinetic analysis in rat ovarian homogenates. *Steroids* 1990; 55:69-73.
111. Krekels MD, Wouters W, De Coster R, Van Ginckel R, Leonaers A, Janssen PA. Aromatase in the human choriocarcinoma JEG-3: inhibition by R 76 713 in cultured cells and in tumors grown in nude mice. *J. Steroid Biochem. Mol. Biol.* 1991; 38:415-422.
112. Wouters W, De Coster R, Beerens D, et al. Potency and selectivity of the aromatase inhibitor R 76,713. A study in human ovarian, adipose stromal, testicular and adrenal cells. *J. Steroid Biochem.* 1990; 36:57-65.
113. Rogol AD, Yesalis CE, 3rd. Clinical review 31: Anabolic-androgenic steroids and athletes: what are the issues? *J. Clin. Endocrinol. Metab.* 1992; 74:465-469.
114. Parkinson AB, Evans NA. Anabolic androgenic steroids: a survey of 500 users. *Med. Sci. Sports Exerc.* 2006; 38:644-651.
115. Abdelgadir SE, Resko JA, Ojeda SR, Lephart ED, McPhaul MJ, Roselli CE. Androgens regulate aromatase cytochrome P450 messenger ribonucleic acid in rat brain. *Endocrinology* 1994; 135:395-401.
116. Roselli CE, Salisbury RL, Resko JA. Genetic evidence for androgen-dependent and independent control of aromatase activity in the rat brain. *Endocrinology* 1987; 121:2205-2210.
117. Roselli CE. The effect of anabolic-androgenic steroids on aromatase activity and androgen receptor binding in the rat preoptic area. *Brain Res.* 1998; 792:271-276.
118. Roselli CE, Resko JA. Androgens regulate brain aromatase activity in adult male rats through a receptor mechanism. *Endocrinology* 1984; 114:2183-2189.
119. Jakab RL, Horvath TL, Leranth C, Harada N, Naftolin F. Aromatase immunoreactivity in the rat brain: gonadectomy-sensitive hypothalamic neurons and an unresponsive "limbic ring" of the lateral septum-bed nucleus-amygdala complex. *J. Steroid Biochem. Mol. Biol.* 1993; 44:481-498.
120. Lisciotto CA, Morrell JI. Sex differences in the distribution and projections of testosterone target neurons in the medial preoptic area and the bed nucleus of the stria terminalis of rats. *Horm. Behav.* 1994; 28:492-502.
121. Mathias LJ, Jacobson NA, Rhees RW, Lephart ED. Brain aromatase in control versus castrated Norway Brown, Sprague-Dawley and Wistar adult rats. *Proc. Soc. Exp. Biol. Med.* 1999; 221:126-130.
122. Estrada M, Uhlen P, Ehrlich BE. Ca2+ oscillations induced by testosterone enhance neurite outgrowth. *J. Cell Sci.* 2006; 119:733-743.
123. Estrada M, Varshney A, Ehrlich BE. Elevated testosterone induces apoptosis in neuronal cells. *J. Biol. Chem.* 2006; 281:25492-25501.
124. Ryan KJ. Biological aromatization of steroids. *J. Biol. Chem.* 1959; 234:268-272.

125. Azcoitia I, Sierra A, Veiga S, Honda S, Harada N, Garcia-Segura LM. Brain aromatase is neuroprotective. *J. Neurobiol.* 2001; 47:318-329.
126. Dewey SL, Smith GS, Logan J, Brodie JD, Fowler JS, Wolf AP. Striatal binding of the PET ligand ^{11}C-raclopride is altered by drugs that modify synaptic dopamine levels. *Synapse* 1993; 13:350-356.
127. Holthoff VA, Koeppe RA, Frey KA, Paradise AH, Kuhl DE. Differentiation of radioligand delivery and binding in the brain: validation of a two-compartment model for [^{11}C]flumazenil. *J. Cereb. Blood Flow Metab.* 1991; 11:745-752.
128. Koeppe RA, Holthoff VA, Frey KA, Kilbourn MR, Kuhl DE. Compartmental analysis of [^{11}C]flumazenil kinetics for the estimation of ligand transport rate and receptor distribution using positron emission tomography. *J. Cereb. Blood Flow Metab.* 1991; 11:735-744.
129. Ichise M, Liow JS, Lu JQ, et al. Linearized reference tissue parametric imaging methods: application to [^{11}C]DASB positron emission tomography studies of the serotonin transporter in human brain. *J. Cereb. Blood Flow Metab.* 2003; 23:1096-1112.
130. Resko JA, Pereyra-Martinez AC, Stadelman HL, Roselli CE. Region-specific regulation of cytochrome P450 aromatase messenger ribonucleic acid by androgen in brains of male rhesus monkeys. *Biol. Reprod.* 2000; 62:1818-1822.
131. Trainor BC, Rowland MR, Nelson RJ. Photoperiod affects estrogen receptor alpha, estrogen receptor beta and aggressive behavior. *Eur. J. Neurosci.* 2007; 26:207-218.
132. Imwalle DB, Gustafsson JA, Rissman EF. Lack of functional estrogen receptor beta influences anxiety behavior and serotonin content in female mice. *Physiol. Behav.* 2005; 84:157-163.
133. Menard CS, Harlan RE. Up-regulation of androgen receptor immunoreactivity in the rat brain by androgenic-anabolic steroids. *Brain Res.* 1993; 622:226-236.
134. Hatsumi T, Yamamuro Y. Downregulation of estrogen receptor gene expression by exogenous 17beta-estradiol in the mammary glands of lactating mice. *Exp. Biol. Med.* 2006; 231:311-316.
135. Kirilovas D, Bergstrom M, Bonasera TA, et al. In vitro evaluation of aromatase enzyme in granulosa cells using a [^{11}C]vorozole binding assay. *Steroids* 1999; 64:266-272.
136. Kirilovas D, Naessen T, Bergstrom M, et al. Effects of androgens on aromatase activity and ^{11}C-vorozole binding in granulosa cells in vitro. *Acta Odontol. Scand.* 2003; 82:209-215.